

Foundations of the rate theory of radiation effects with account of non-linear excitations in crystals

V.I. Dubinko



OUTLINE

1. Driving forces of microstructure evolution
2. Early Rate Theory of the radiation-induced void swelling
3. Experimental verification of dislocation bias: unsolved puzzle!
4. Radiation-induced formation of Schottky defects:
MD simulations and **Modified Rate Theory**
5. Non-linear effects: **D**iscrete **B**reathers and **Q**uodons: definition and discovery: insulators and metals
6. Applications in physics of radiation effects:
7. **Modified Rate Theory of swelling**
Radiation-induced “**annealing**” of voids
Swelling saturation and ordering of voids

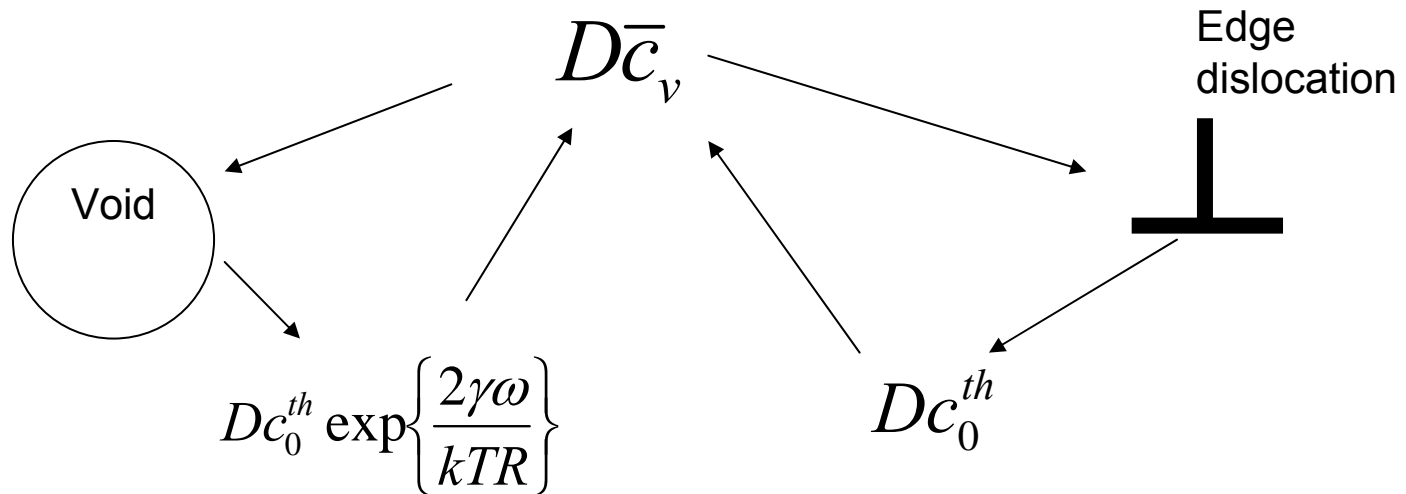
Radiation-induced void swelling

1.2 MeV Cr³⁺ → Ni (600°C, ~25 dpa) DOSE RATE: 7×10^{-3} dpa / s



Driving forces of microstructure evolution

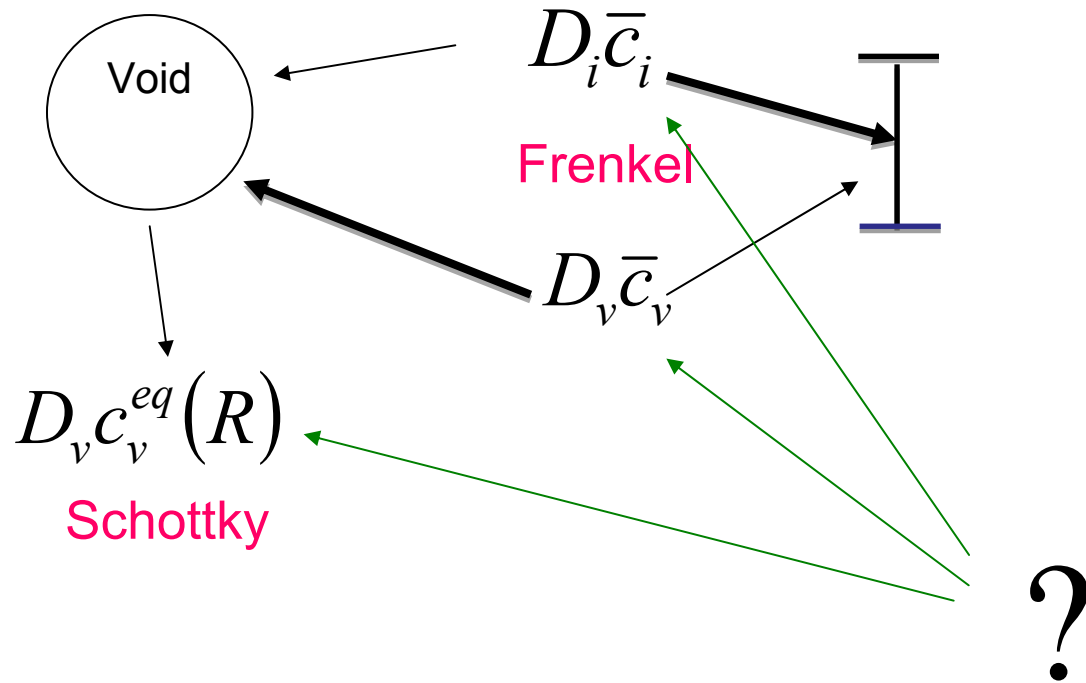
Thermal treatment
(only Schottky defects)



$$Dc_0^{th} \propto \exp\left(-\frac{E_v^m + E_v^f}{kT}\right)$$

- Arrhenius' law – how universal is it?

Driving forces of microstructure evolution
under irradiation:
Frenkel and Schottky defect production



Rate theory of crystal defects under irradiation

(1) Schottky + Frenkel defects

Rate equations:

$$\frac{d\bar{c}_i}{dt} = K_{FP}(1 - \varepsilon_i) - k_i^2 D_i \bar{c}_i - \beta_r (D_i + D_v) \bar{c}_i \bar{c}_v,$$

$K_{FP} = k_{eff} K$ - Frenkel pair production rate

$$\frac{d\bar{c}_v}{dt} = K_{FP}(1 - \varepsilon_v) - k_v^2 D_v \bar{c}_v - \beta_r (D_i + D_v) \bar{c}_i \bar{c}_v + k_v^2 D_v \bar{c}_v^{eq}$$

Schottky defect production rate

$$k_{i,v}^2 = Z_{i,v}^d \rho_d + Z_{i,v}^V 4\pi N_V \bar{r}_V + \dots$$
 - Microstructure sink strength

Steady-state conditions:

$$D_v \bar{c}_v = \frac{k_i^2}{k_v^2} D_i \bar{c}_i + D_v \bar{c}_v^{eq} \Rightarrow D_v \bar{c}_v \approx D_i \bar{c}_i \Rightarrow$$

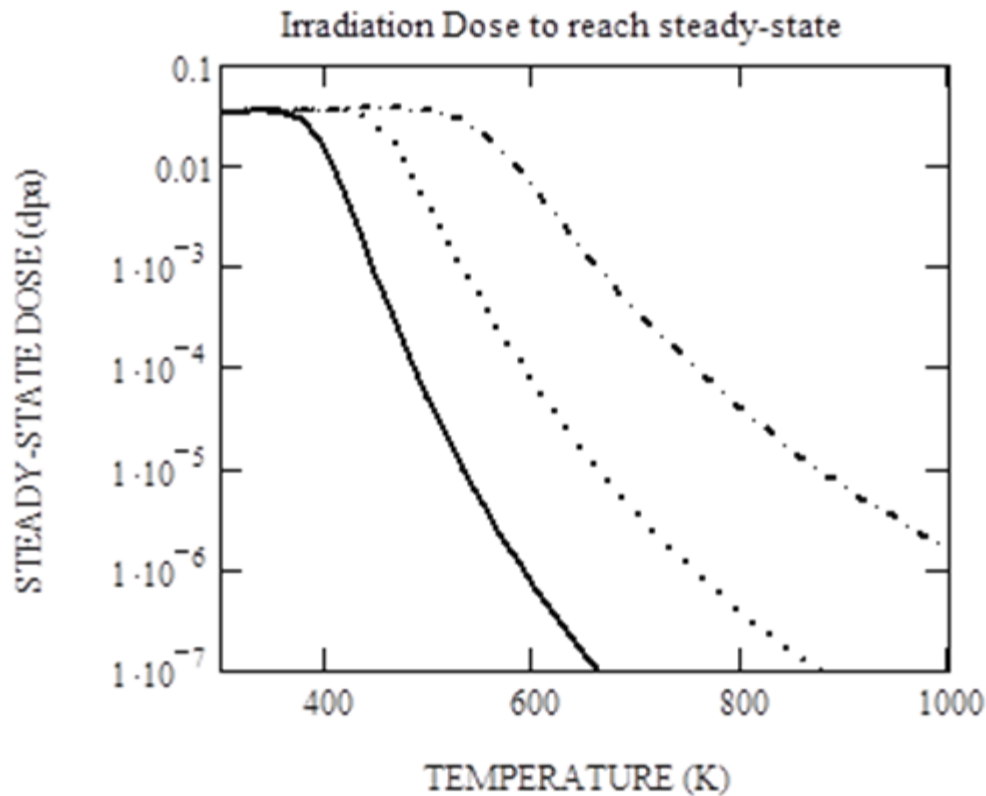
Bias factors are important, not the defect diffusivities !

Bias factor of a straight edge dislocation (Ham, 1959):

$$B_D = \frac{Z_i^d - Z_v^d}{Z_v^d} \approx \frac{\ln(\Omega_i / |\Omega_v|)}{2\pi \ln(2R_{di} / L_i)}$$

$$R_{di} \approx \frac{1}{k_i}, \quad L_n = \frac{\mu b(1 + \nu) |\Omega_n|}{3\pi k T(1 - \nu)},$$

Irradiation dose required to reach steady-state



- K=10⁻⁶ dpa/s
- K=10⁻⁴ dpa/s
- · - · K=10⁻² dpa/s

$$K t_{steady} \approx (D_v k_v^2)^{-1}$$

$$D_v \bar{c}_v = \frac{k_i^2}{k_v^2} D_i \bar{c}_i + D_v \bar{c}_v^{eq} \Rightarrow D_v \bar{c}_v \approx D_i \bar{c}_i \Rightarrow$$

Rate theory of crystal defects under irradiation

(2) Absorption dislocation bias factor and swelling rate

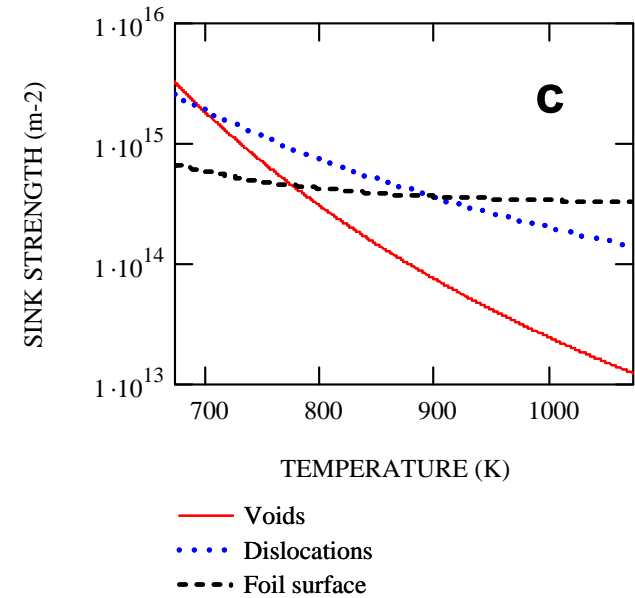
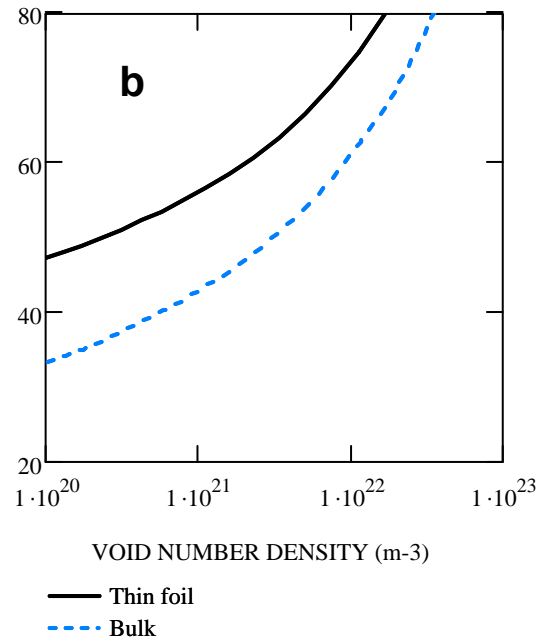
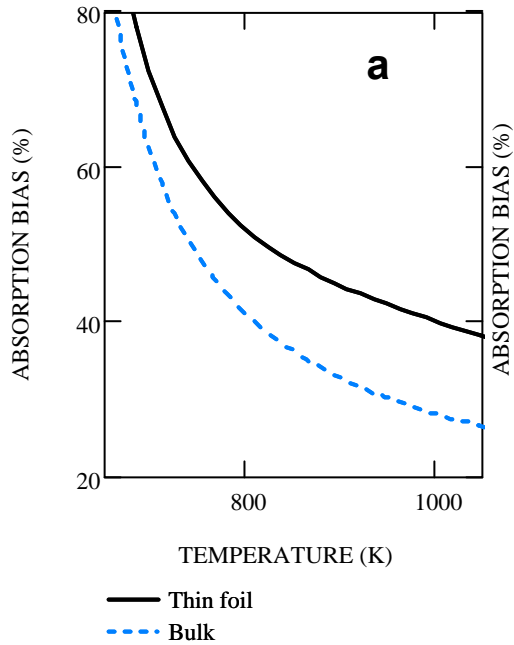
$$\frac{dS}{dt} = 4\pi N_V \bar{R}_V^2 \frac{dR_V}{dt} = D_i \bar{c}_i \frac{k_{Vv}^2 k_{dv}^2}{k_v^2} B_{ab} - D_v \frac{k_{Vv}^2 k_{dv}^2}{k_v^2} (c_{vV}^{eq} - \bar{c}_v^{eq})$$

$$B_{ab} \equiv \frac{Z_v^V Z_i^d - Z_i^V Z_v^d}{Z_v^d} + \frac{Z_v^V k_{Gi}^2 - Z_i^V k_{Gv}^2}{Z_v^d \rho_d}$$

$$B_{ab} \xrightarrow{R_V \rightarrow \infty, dg \times \rho_d \rightarrow \infty} \frac{Z_i^d - Z_v^d}{Z_v^d} \equiv B_d$$

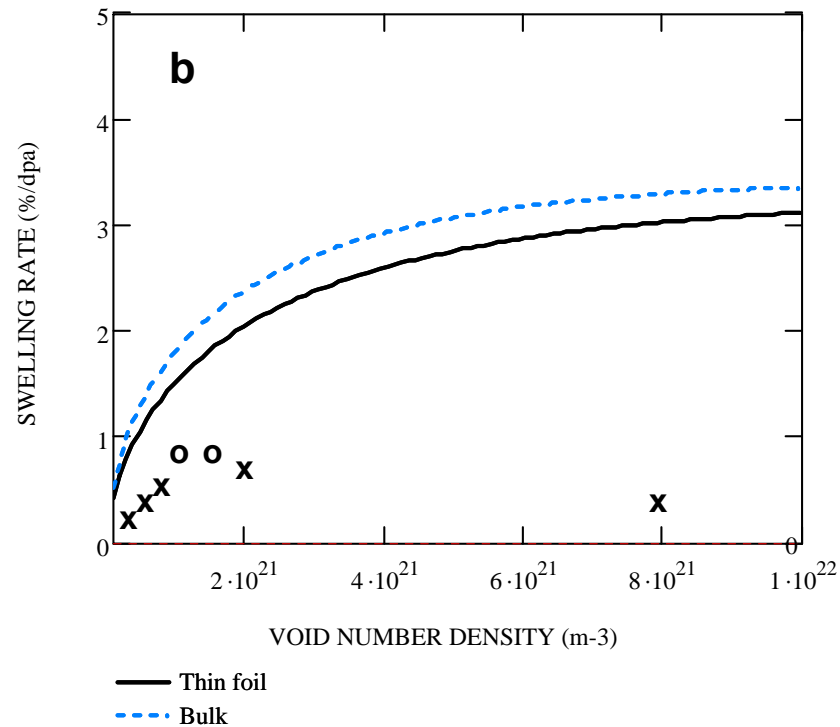
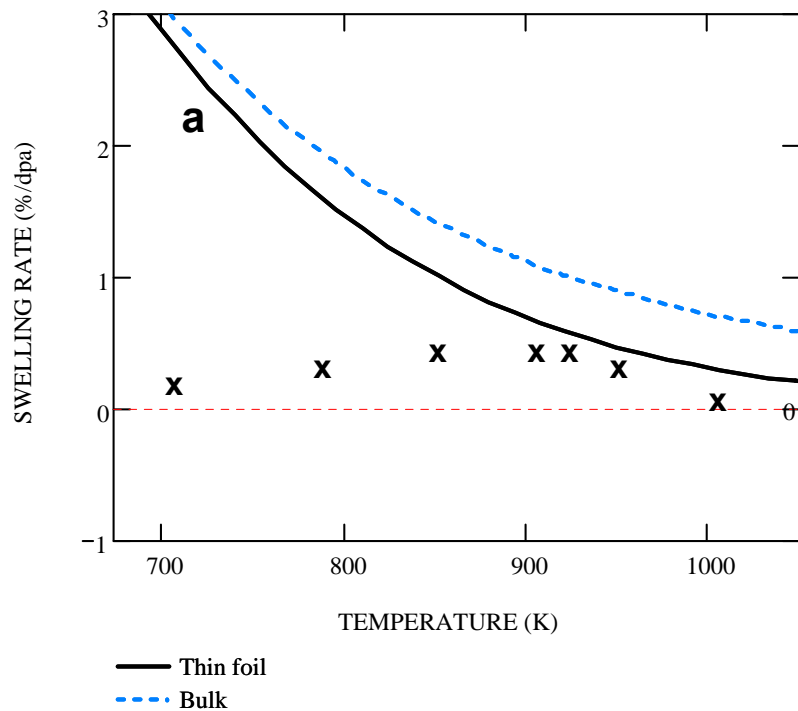
Experimental evaluation of dislocation bias

Makin et al. JNM (1980 -1985)



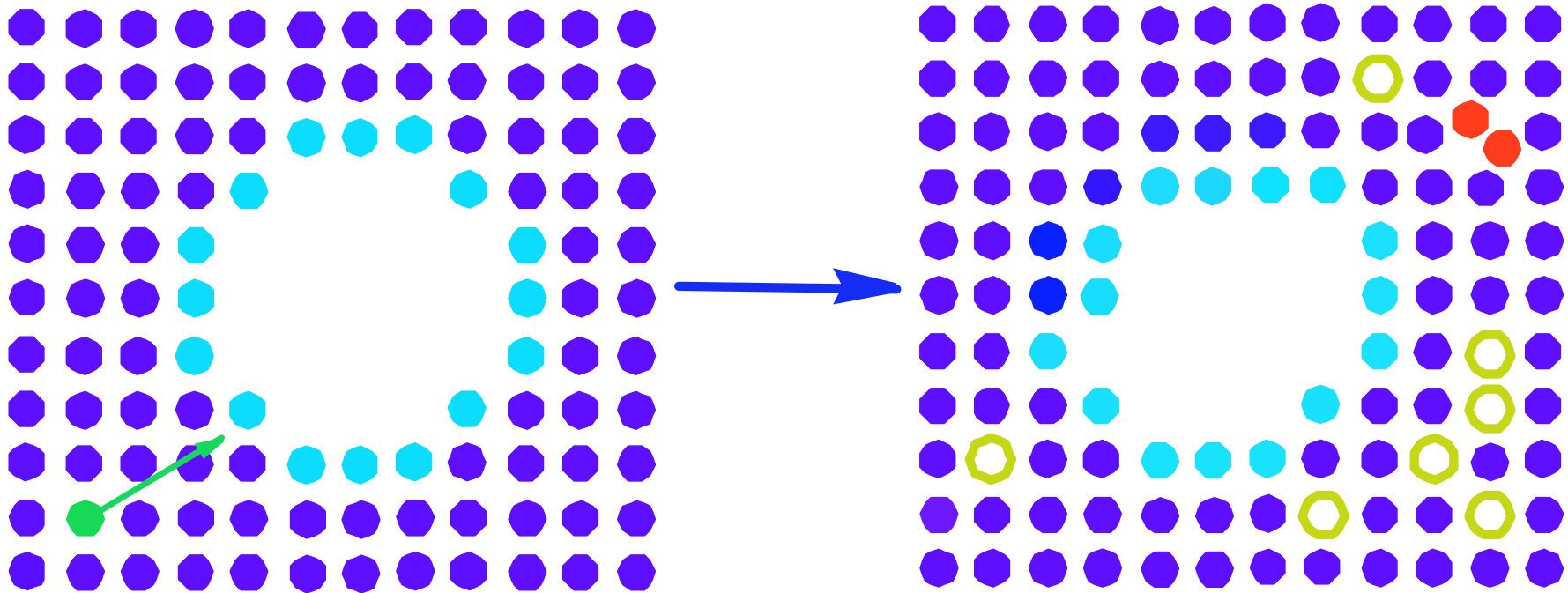
Absorption bias calculated using the experimental data (c) as a function of temperature (a) and the void number density (b)

Evaluation of swelling rate in early FP3DM and comparison with experimental data Makin et al. JNM (1980 -1985)



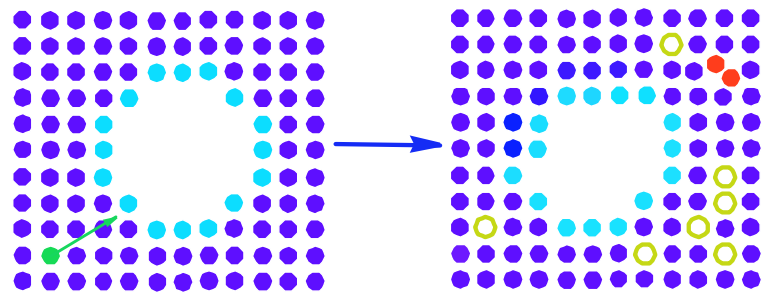
Swelling rate calculated as a function of temperature and the void number density. Experimental data for austenitic steel (a) and for a pure Fe-Ni-Cr alloy (b), where **x** and **o** represent residual gas and 10 appm pre-injected helium

Radiation-induced formation of Schottky defects



Schematic representation of point defect formation near a void. The size of void corresponds to about 300 atomic volumes. PKA ranges of 2 - 10 interatomic distances from the void surface.

MD simulation of point defects production in the vicinity of extended defects



Schematic representation of point defect formation near a void.
 N. P. Lazarev, V. I. Dubinko,
 Radiat. Eff. Def. Solids 158 (2003) 803

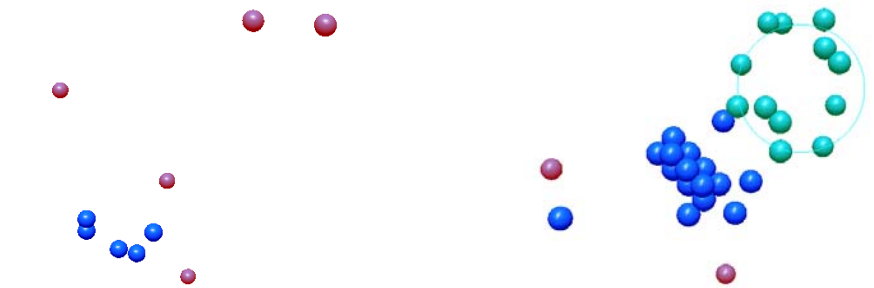
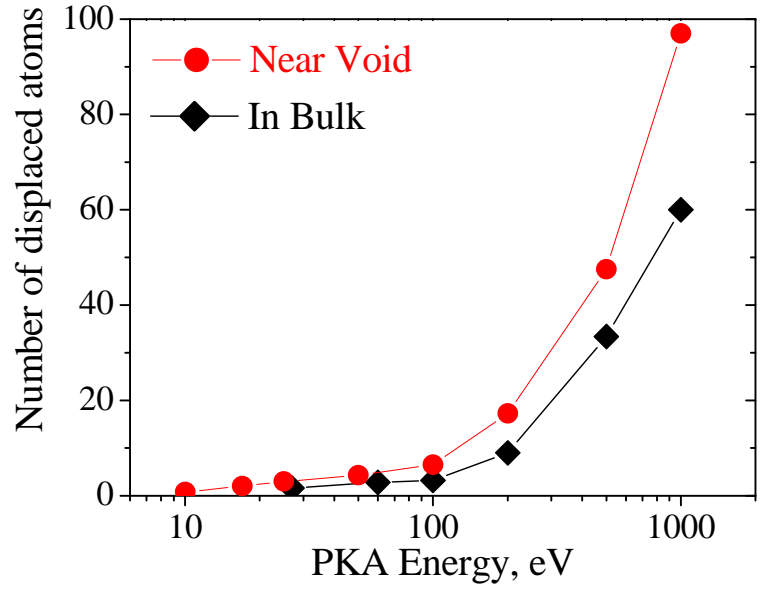
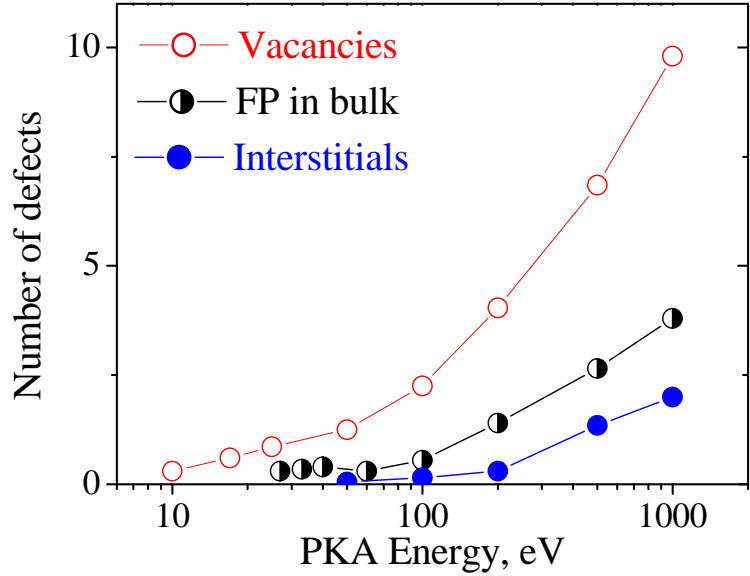
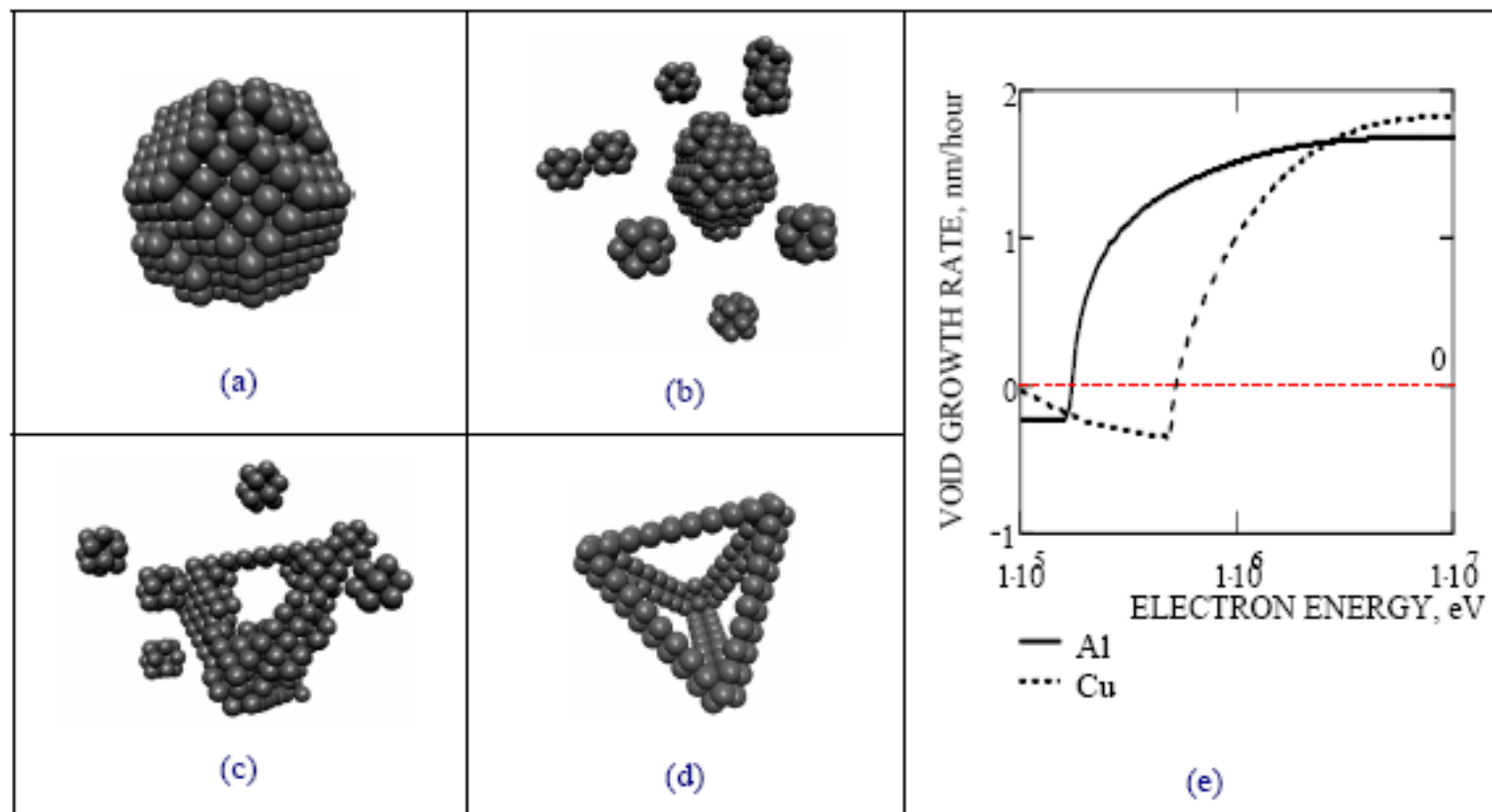


Illustration of the final stages of collision cascade developments in the bulk (left) and near the void (right) at PKA energy 1 keV.



In contrast to the Frenkel pair production in the bulk, the collision events in the vicinity of extended defects results in a *biased* formation of *vacancies* due to the lower energy barrier involved

DISSOLUTION OF VOIDS BY SUBTHRESHOLD IRRADIATION



Different stages of the void dissolution. The atoms are shown, which coordination numbers are less than 12. (a) The void initial size is 312ω ; (b) After 37 ns of the simulation and 765 collision cascades activated; (c) Beginning of the stacking fault tetrahedron (SFT) formation after 72 ps. (d) Final state of the SFT development; (e) Calculated void growth rate vs. electron beam energy at 200°C , $j_e = 10^{19}\text{ cm}^{-2}\text{s}^{-1}$, $l_e = 1\mu$,

Radiation-induced solubility limit

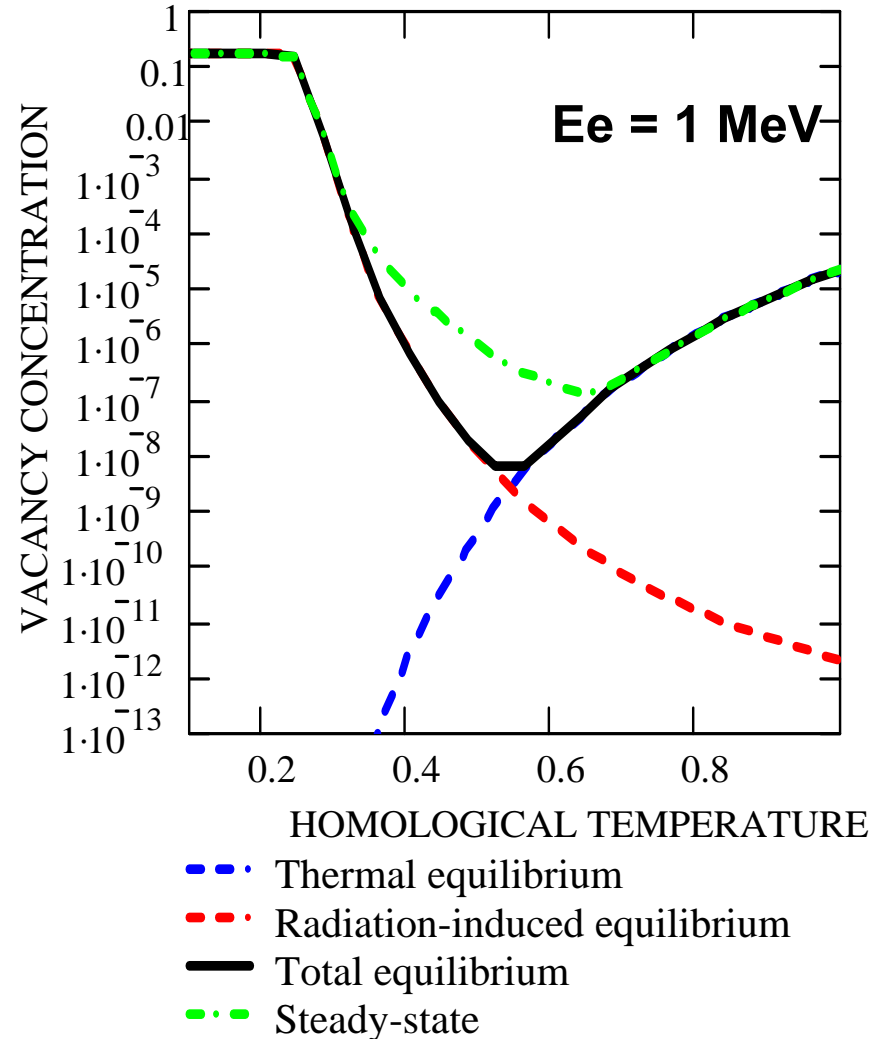
$$c_v^{eq}(T, K) = c_v^{th}(T) + c_v^{irr}(T, K)$$

$$c_v^{th}(T) = \exp\left(-\frac{E_v^f}{k_B T}\right)$$

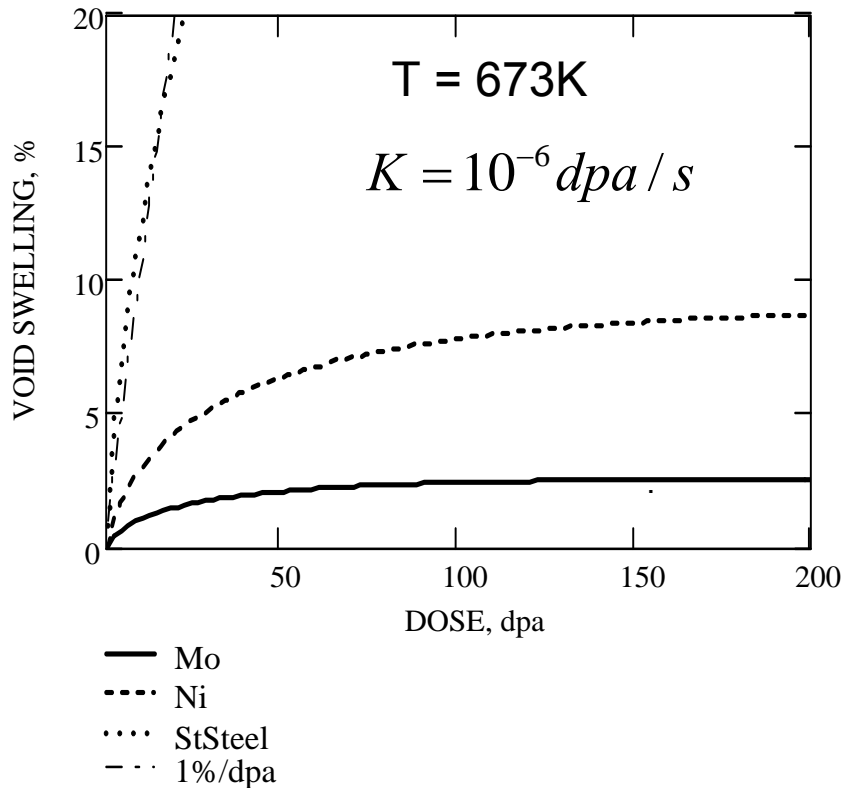
$$c_v^{irr}(T, K) \approx \frac{Kbl_{irr}}{D_v(T, K)} \frac{E_d}{E_F} \Phi(E_v^{SD}, E_F)$$

$$\Phi(E_v^{SD}, E_F) = \int_1^{E_v^{SD}/E_F} \ln x \ln\left(x \frac{E_F}{E_v^{SD}}\right) dx$$

$$E_v^{SD} = E_v^f + E_v^m \quad \text{Self-diffusion activation energy}$$



Swelling saturation with increasing irradiation dose



Dose dependence of swelling in metals with different void number densities, N_V

Mo $N_V = 2 \times 10^{16} \text{ cm}^{-3}$

Ni $N_V = 8 \times 10^{15} \text{ cm}^{-3}$

St steel $N_V = 2 \times 10^{15} \text{ cm}^{-3}$

Focuson range $l_F^0 = 100 \text{ b}$

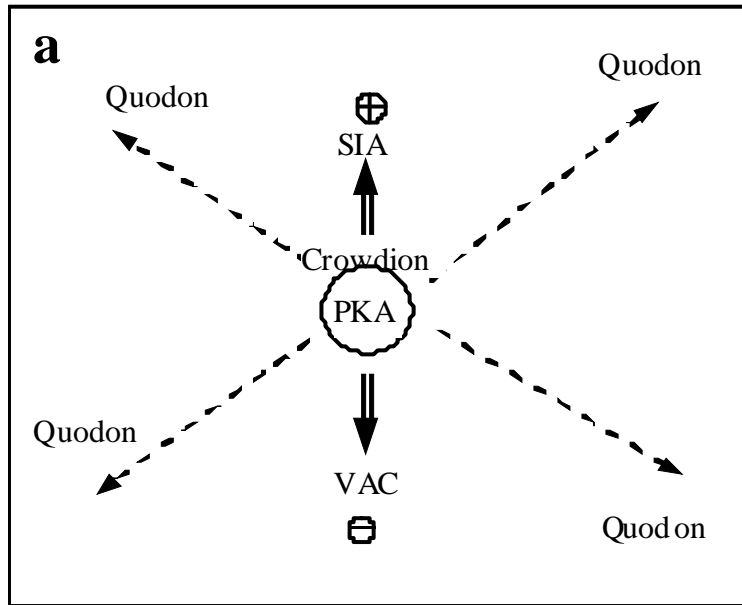
Formation energy difference $\Delta E_d \approx 4eV$

Why Non-linear effects ?

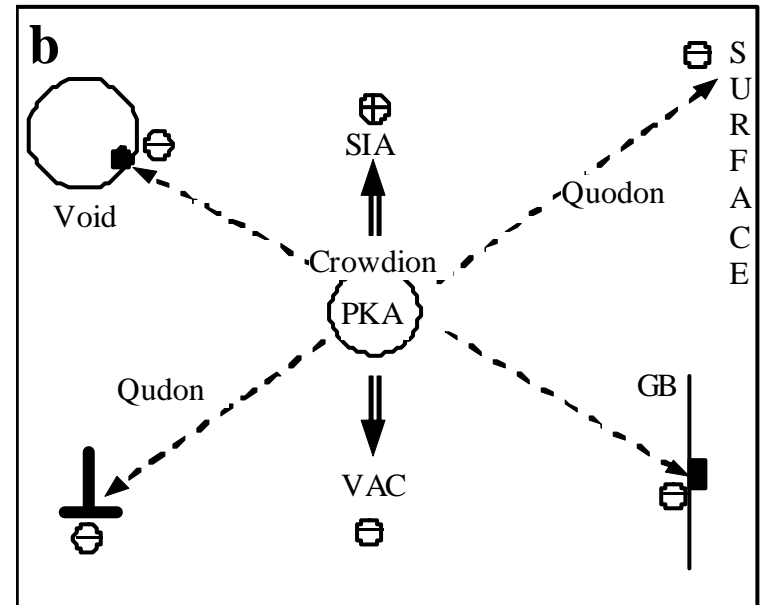
Focusons are unstable against thermal motion because they depend on the alignment of atoms. Typically, at elevated temperatures, **the focuson range is limited to several unit cells** and their lifetime is measured in picoseconds. However, there exists much more powerful, **essentially non-linear**, lattice excitations having large lifetimes and **huge propagation distances**, which are called discrete breathers (DBs) or intrinsic localized modes (ILMs) and quodons

Frenkel and Schottky defect production by Crowdions and Quodons

Perfect crystal



Crystal with EDs

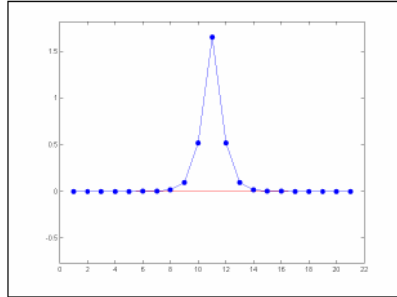


Nonlinear coupled oscillators



$$V = \sum V(X_n) + C W(X_n, X_{n+1})$$

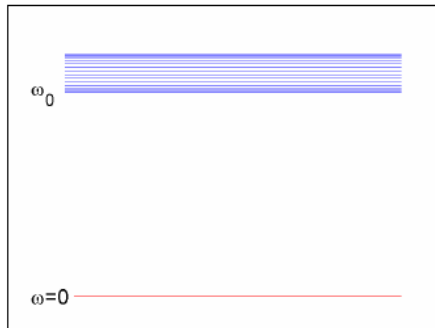
- Exact, periodic and localized solution



R. S. MacKay; S. Aubry, *Proof of existence of breathers for time-reversible or Hamiltonian networks of weakly coupled oscillators*, Nonlinearity 7, 1623 (1994)

Phonons

- Frequency band $\omega_{ph}^2 = \omega_0^2 + 4C \sin^2 q/2$
- Non localized states

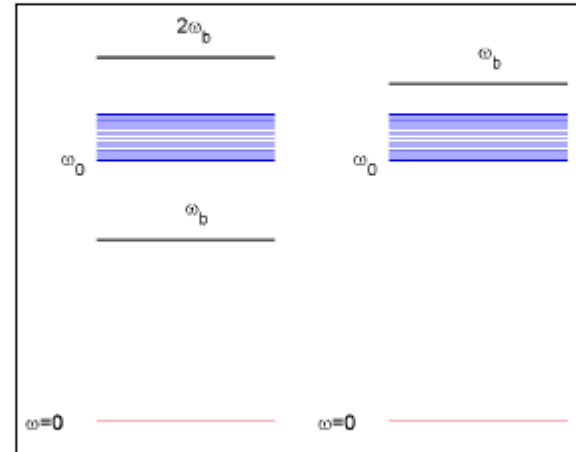


Existence of breathers (1994)

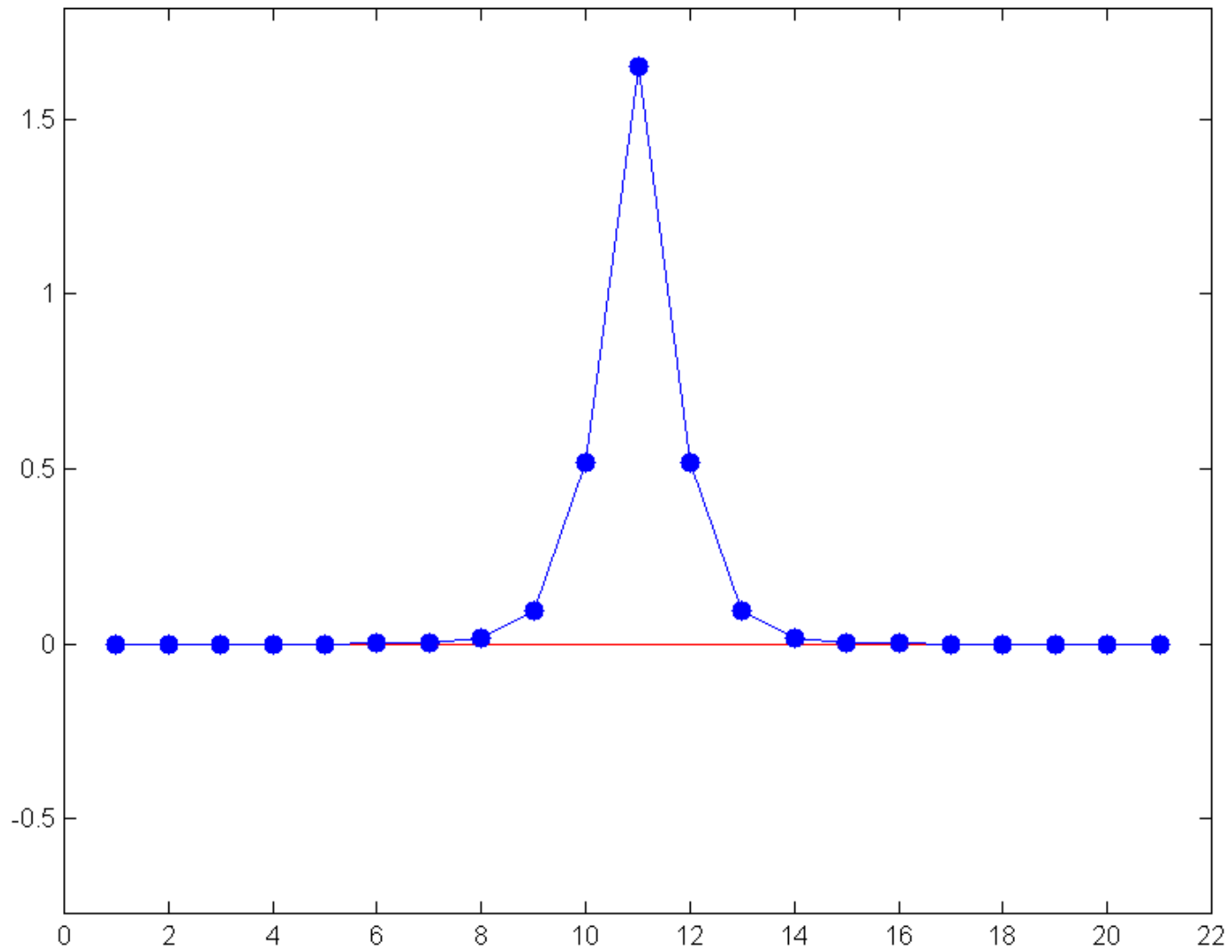


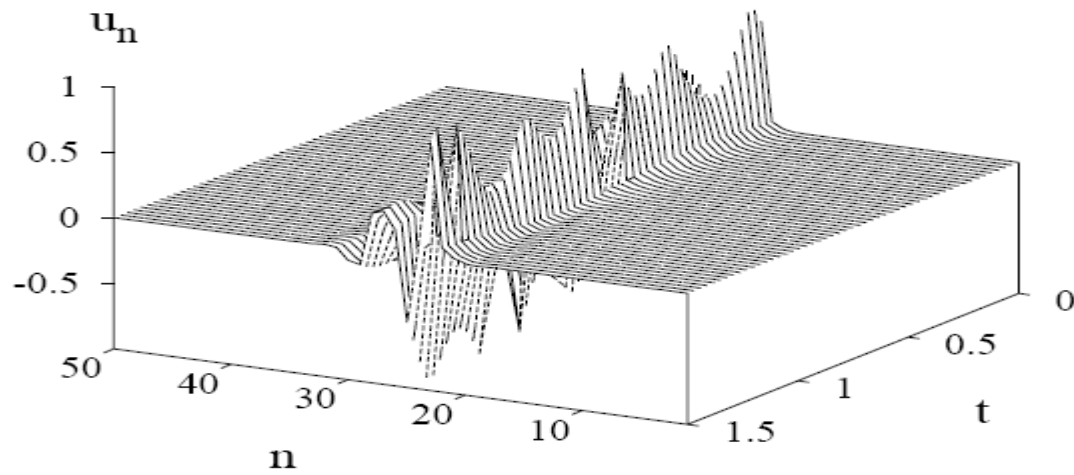
Soft

Hard



$$\text{if } \omega_b \notin [\omega_0, \omega_{f,\text{máx}}], \quad \omega_b'(E) \neq 0$$





Discrete breathers in anharmonic lattice

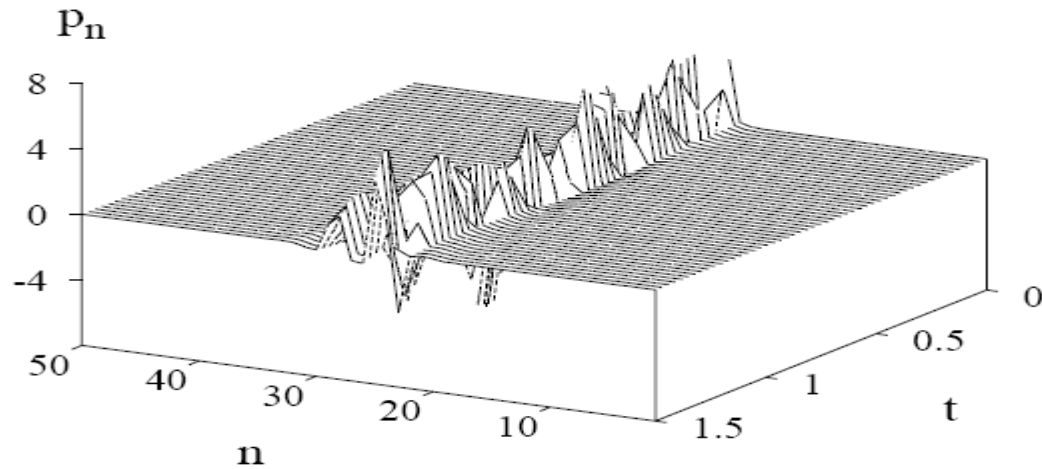
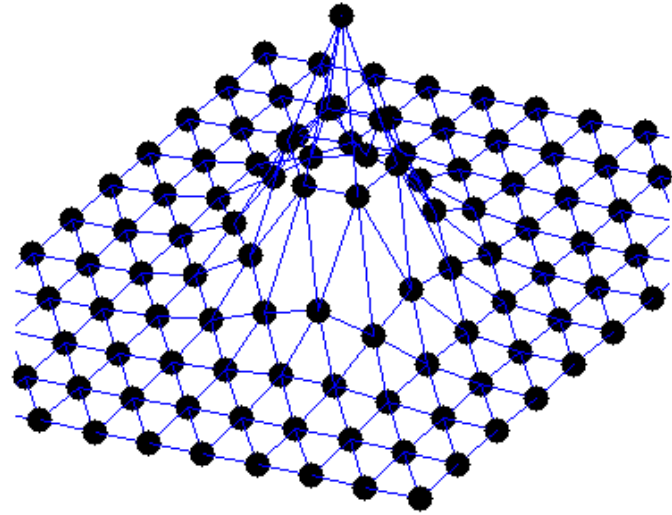


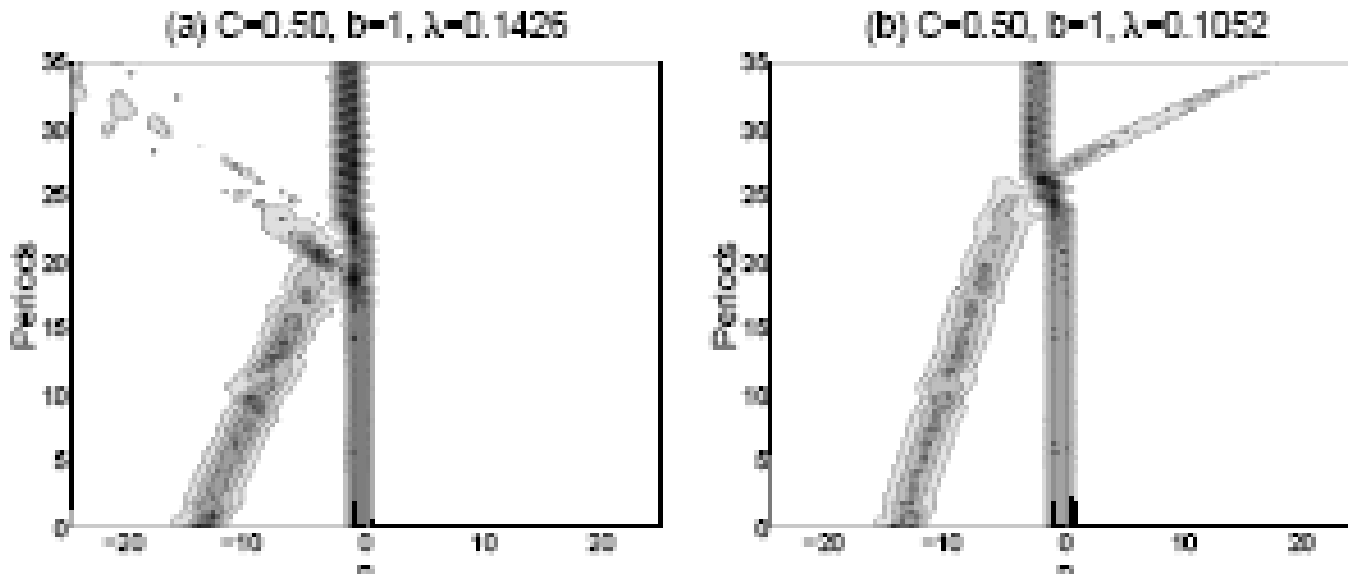
Fig. 5. Time dependence, in picoseconds, of the lattice displacement, u_n , in \AA , and momenta, p_n , in $M \cdot \text{\AA}/\text{ps}$, of site n . The system parameters are as in Fig. 1. The initial momenta are defined as $p_n(0) = 5.27526M(u_n - u_{n-1})$.



Discrete breathers can move and transport coherently energy through the lattice:

Interaction of moving discrete breathers with

vacancies, J Cuevas, JFR Archilla, B S´anchez-Rey, FR Romero, 2005



Energy density plot for the interaction moving breather–vacancy. The particle to the right of the vacancy is located at $n = 0$. In (a), the moving breather is reflected and the vacancy moves backwards, in (b) the breather is transmitted and the vacancy moves backwards.

Uranium Atoms Don't Share the Vibe



[Phys. Rev. Lett. 96, 125501](#)

(issue of 31 March 2006)

C.P. Opeil, S.J./Los Alamos National Lab

Hot material. Experiments on this uranium crystal at high temperatures show that a few atoms can vibrate for a long time without disturbing neighboring atoms. The effect has never been conclusively seen in a **three-dimensional crystal**.

All crystals display some nonlinearity at high enough temperatures, but DBs had only shown up clearly in one- or two-dimensional systems.

Uranium crystals seem to contain many DBs if heated past 450 K.

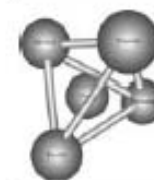
"These sort of things should exist all over the place in materials; it's just really hard to see them," says Michael Manley of Los Alamos National Laboratory .



Available online at www.sciencedirect.com



Acta Materialia 58 (2010) 2926–2935



Acta MATERIALIA

www.elsevier.com/locate/actamat

Impact of intrinsic localized modes of atomic motion on materials properties

M.E. Manley *

Lawrence Livermore National Laboratory, Livermore, CA 94551, USA

Received 1 October 2009; accepted 18 January 2010

Available online 13 February 2010

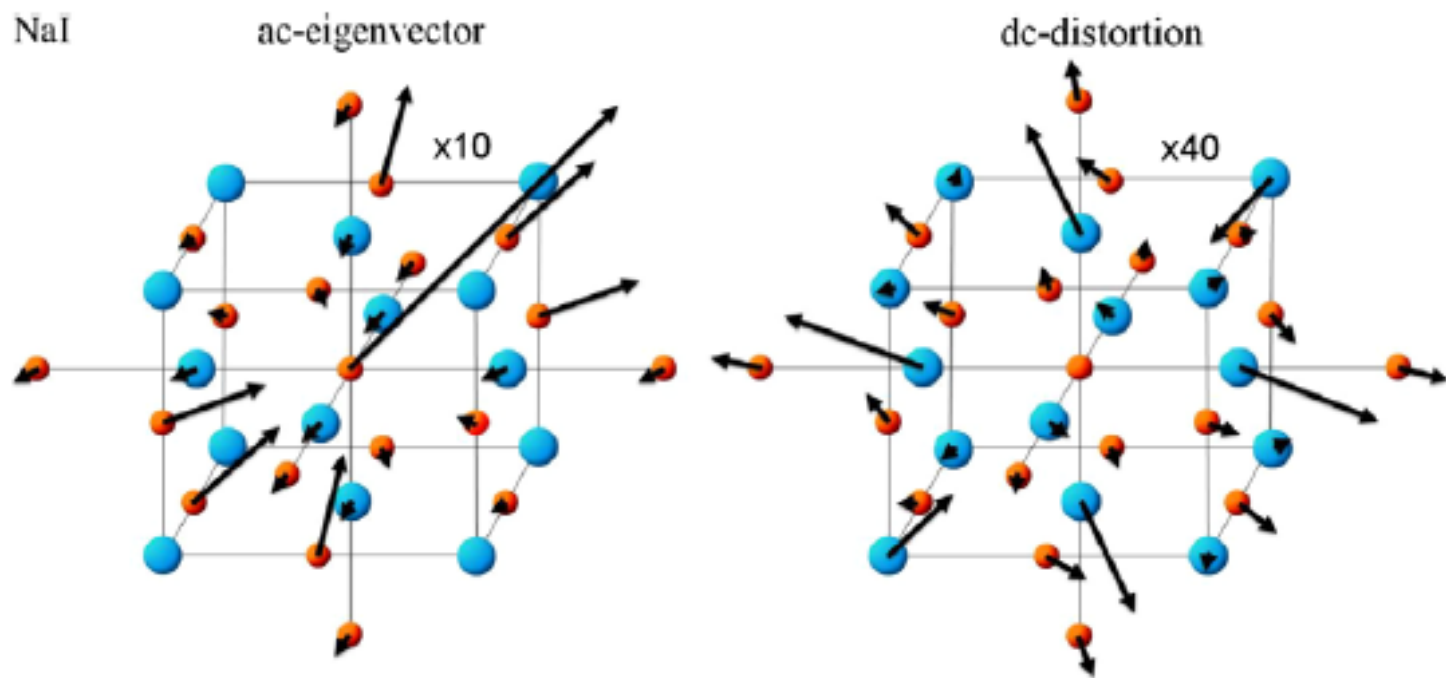


Fig. 1. Eigenvectors of the oscillatory motion, “ac”, and static distortion, “dc”, of an ILM simulated using model potentials for NaI, after Ref. [13]. The small atoms are Na and the large atoms are I. The ILM oscillations, centered at Na, are polarized along the $[1\ 1\ 1]$ direction. The local dc distortions include a contraction along the direction such that the mode displaces atoms in oscillatory motion, and an expansion in the orthogonal direction.

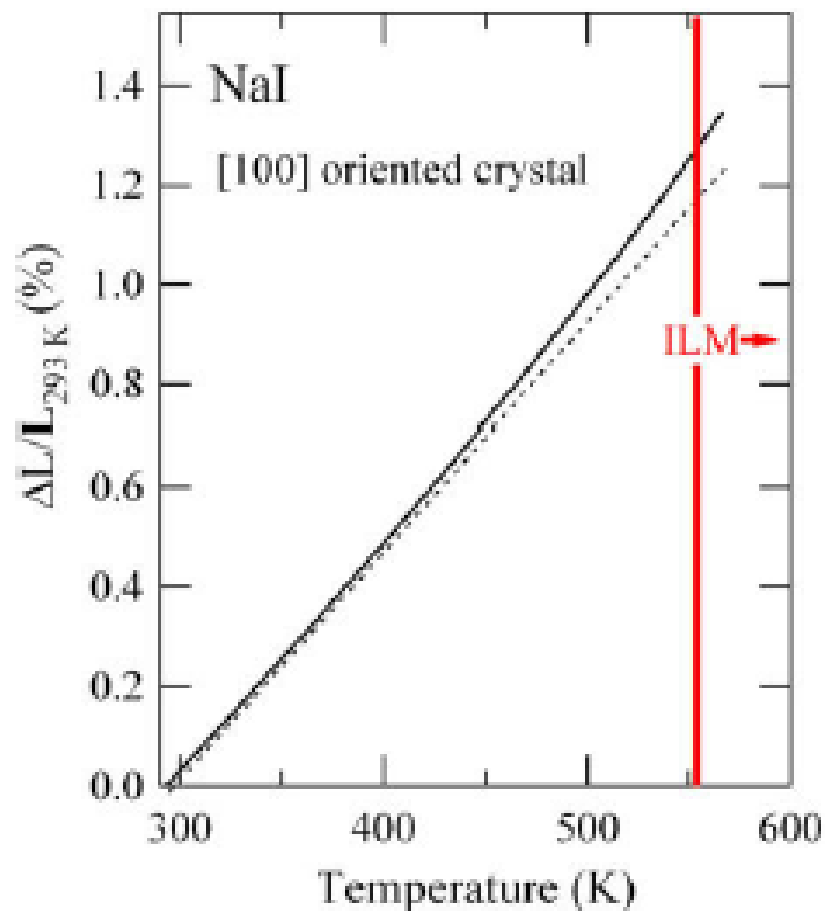


Fig. 2. Thermal expansion of NaI as measured from the dilation of a single crystal along the [1 0 0] direction, after Ref. [14].

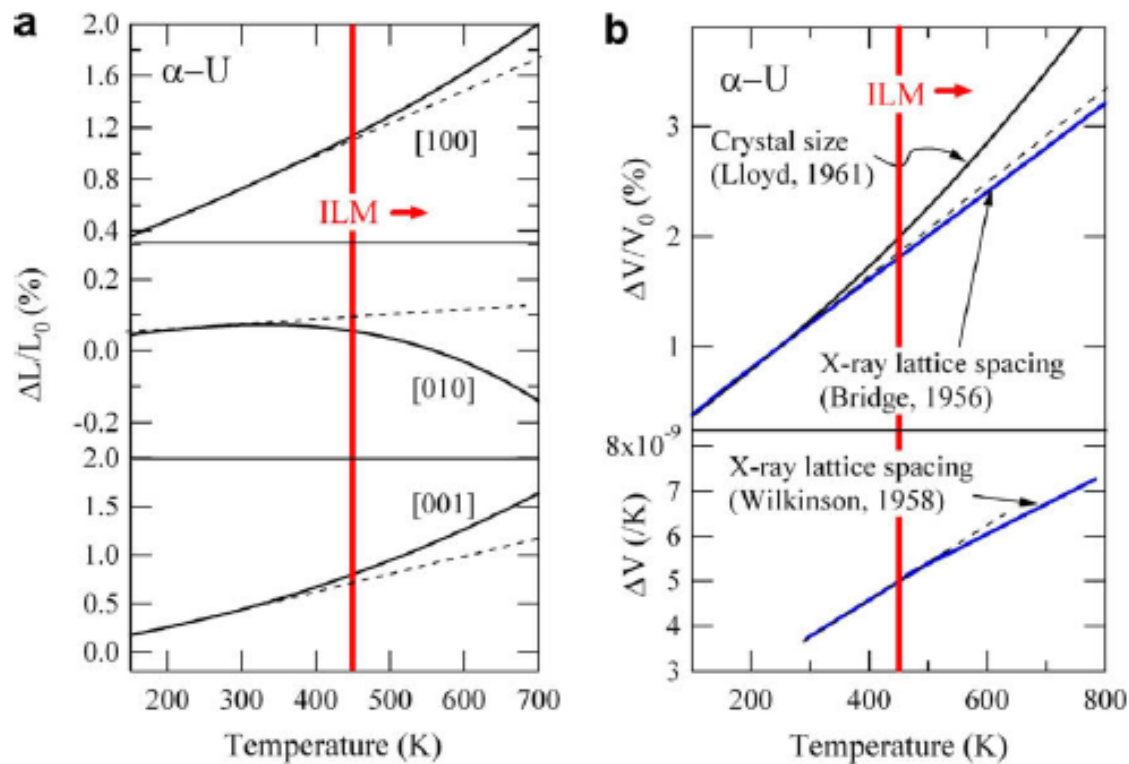


Fig. 3. Thermal expansion of α -U. (a) Per cent length change along the three principle axes of a single crystal measured by Lloyd [15]. (b) Per cent change in volume determined from the single crystal data of Lloyd [15] (solid black line in top panel), and determined from X-ray diffraction determined lattice spacing by Bridge et al. [17] (blue line top panel) and Wilkinson [18] (blue line bottom panel). The ILM activation temperature is indicated by the vertical red line.

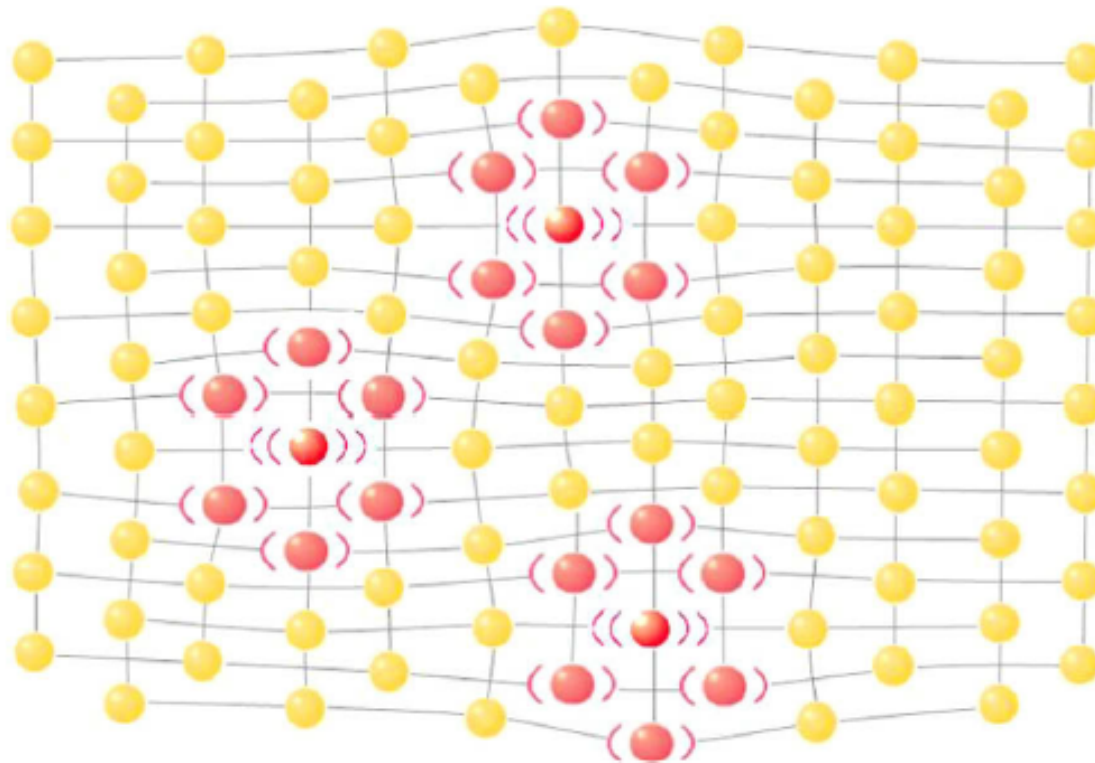


Fig. 4. Simplified illustration of how ILMs may manifest as an inhomogeneous distribution of both lattice vibrational energy and anharmonic thermal expansion. The focusing of the lattice dynamic energy is accompanied by a concomitant focusing of the thermal expansion effect in localized regions.

Symmetry-breaking dynamical pattern and localization observed in the equilibrium vibrational spectrum of NaI

M. E. Manley¹, D. L. Abernathy², N. I. Agladze³ & A. J. Sievers³

¹Lawrence Livermore National Laboratory, Livermore, California 94551, USA, ²Oak Ridge National Laboratory, Oak Ridge, Tennessee 37831, USA, ³Laboratory of Atomic and Solid State Physics, Cornell University, Ithaca, New York 14853-2501, USA.

Intrinsic localized modes (ILMs) – also known as discrete breathers – are localized excitations that form without structural defects in discrete nonlinear lattices. For crystals in thermal equilibrium ILMs were proposed to form randomly, an idea used to interpret temperature activated signatures of ILMs in α -U and NaI. Here, however, we report neutron scattering measurements of lattice vibrations in NaI that provide evidence of an underlying organization: (i) with small temperature changes ILMs move as a *unit* back-and-forth between [111] and [011] orientations, and (ii) when [011] ILMs lock in at 636 K the transverse optic (TO) mode *splits* into three modes with symmetry-breaking dynamical structure resembling that of a superlattice, but there are no superlattice Bragg reflections and the pattern itself has crystal momentum. We conclude that this dynamical pattern is not derived from the rearrangement of atoms but from a coherent arrangement of ILMs decorating the crystal lattice in equilibrium.

Received
20 January 2011

Accepted
21 March 2011

Published
14 June 2011

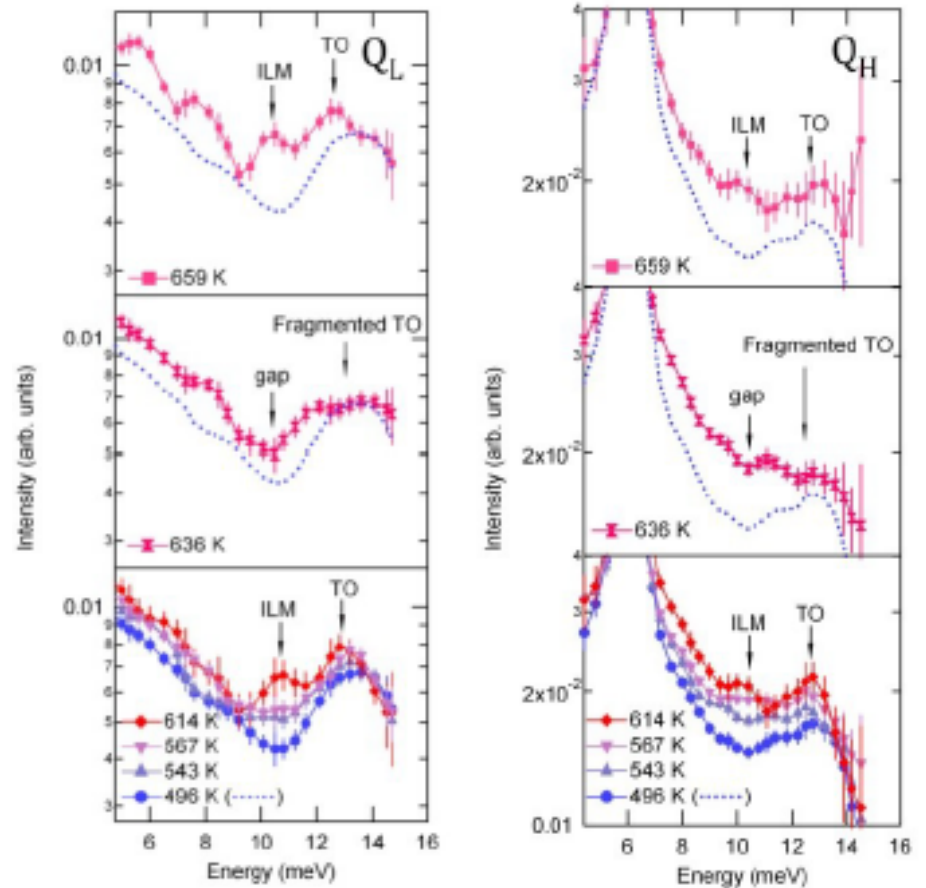
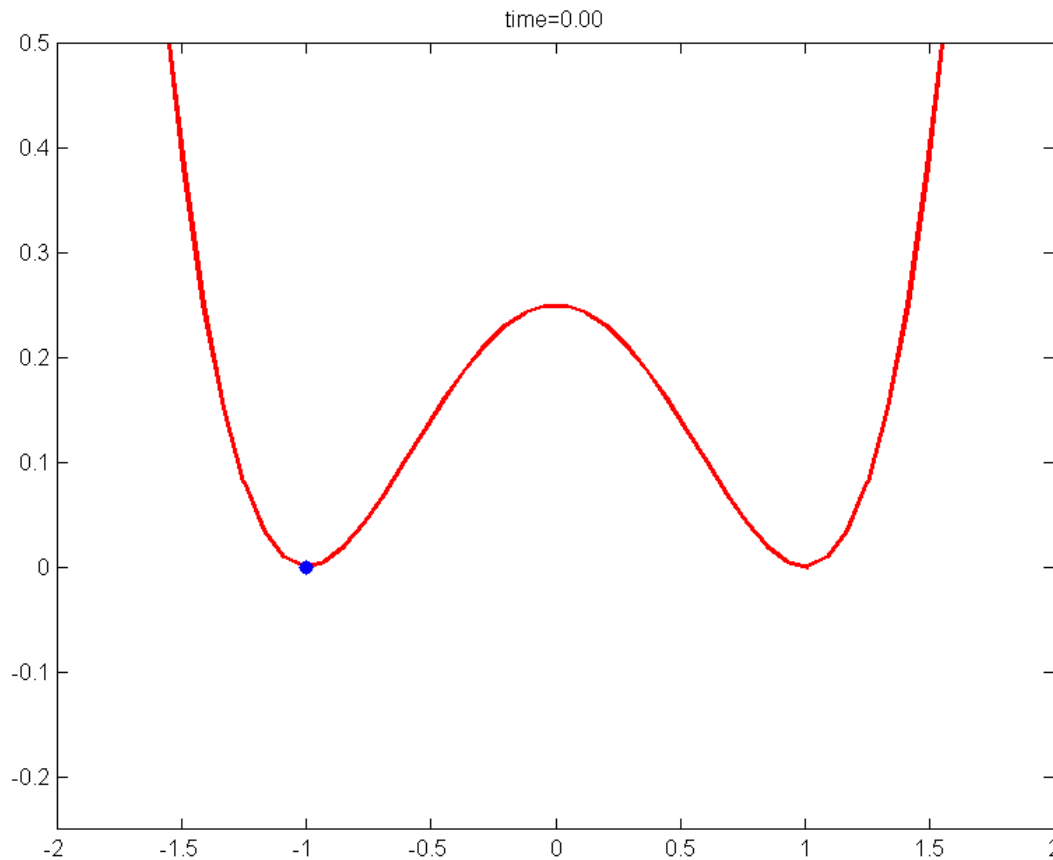


Figure 1 | Lattice excitation spectra derived from a curved section of momentum-energy (Q-E) space as a function of temperature. The Q space sampled in these spectra changes with E. The curved dashed-line section in the pictures above the data sets shows where the detector banks are projected in the NaI reciprocal lattice for energies between 9 meV and 11 meV (where the ILM feature forms⁵). The grey outlined boxes with Q labels indicate the volume of Q

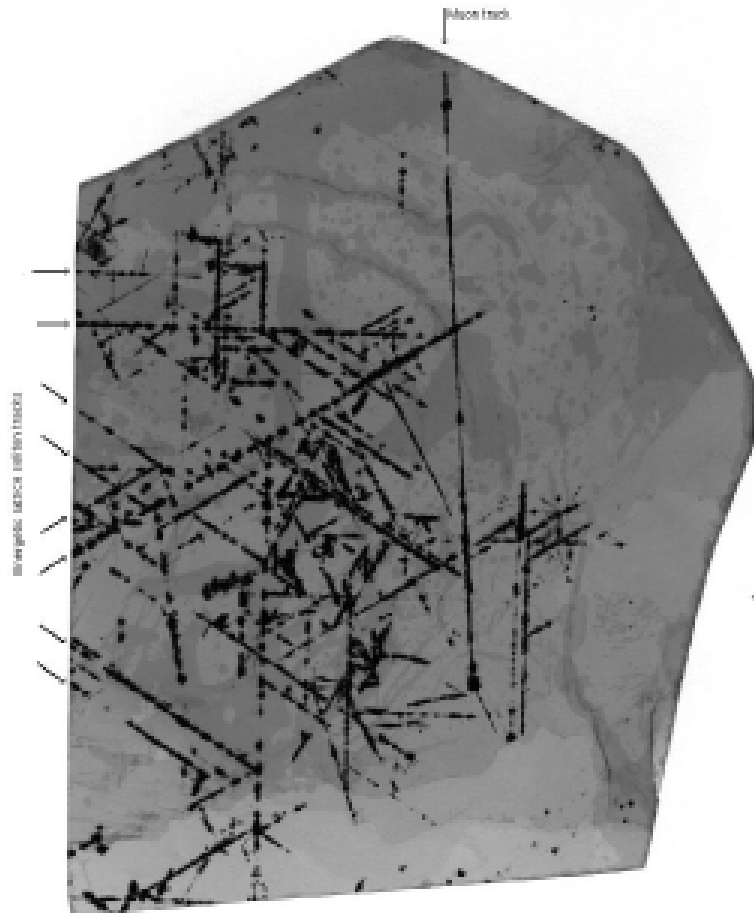
Breather effect: periodic in time modulation of the potential barrier (1)



Quodon definition

As the incident focuson energy is dispersed but the available kinetic energy still far exceeds that of phonons, atoms experience large displacements from their equilibrium positions. Propagation of the corresponding lattice vibrations are governed by nonlinear forces. This may result in formation of vibrational particle-like solitons, called **quodons**. According to molecular dynamic simulations, **quodons** are mobile, highly anharmonic longitudinal vibrations that are sharply localized in longitudinal direction and practically across one atomic distance in the transverse direction. The main difference between **focusons** and **quodons** is that the latter are stable against thermal motion.

Quodons in mica moscovite F.M. Russell



Black tracks: Fe_3O_4

Cause:

- 0.1% Particles:

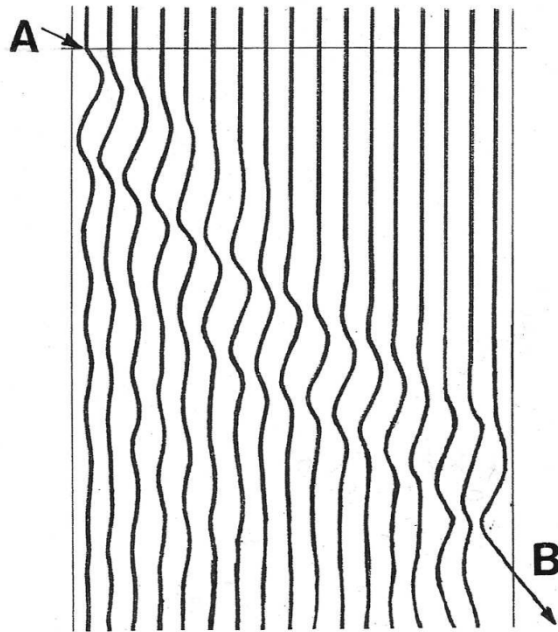
- muons: produced by interaction with neutrines
- Positrons: produced by muons' electromagnetic interaction and K decay

- 99.9% **Unknown**

¿Lattice localized vibrations: quodons?

Mike Russell (center), Juan Archilla (right) and Vladimir Dubinko (left) at Mike's lab (Abingdon, UK, March 2011).





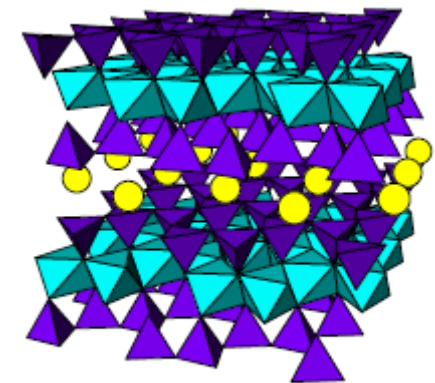
Sputtering



Trayectorias along lattice directions within the K^+ layer

Evidence for moving breathers in a layered crystal insulator at 300K
FM Russell and JC Eilbeck, Europhysics Letters 78, 10004, 2007.

Ejection of atoms at a crystal surface caused by energetic breathers which have travelled more than 10^7 unit cells in atomic chain directions. The **breathers** were created by bombardment of a crystal face with heavy ions. This effect was observed at 300K in the layered crystal muscovite, which has linear chains of atoms for which the surrounding lattice has C2 symmetry.



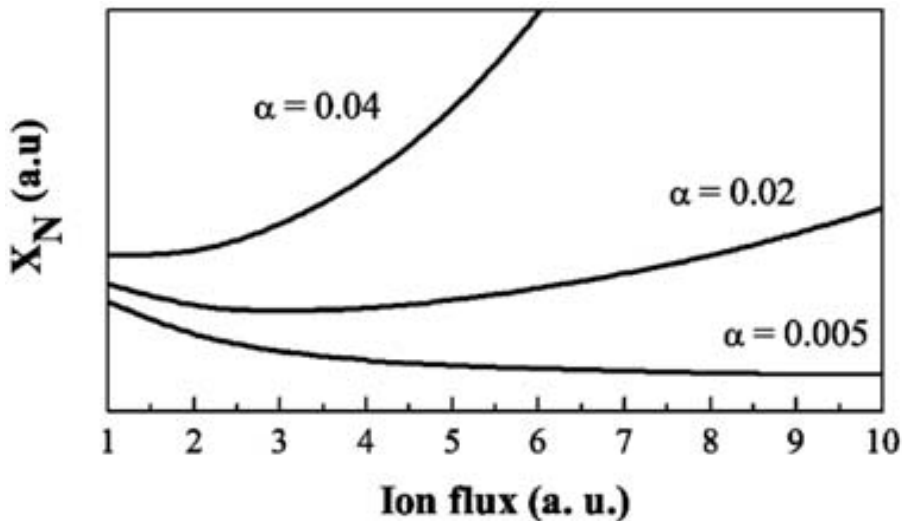
● K^+

Anomalous Ion Accelerated Bulk Diffusion of Interstitial Nitrogen

Gintautas Abrasonis* and Wolfhard Mo"ller

(Received 19 August 2005; published 13 February 2006)

Interstitial N diffusion under low energy (700 eV) Ar bombardment at 673 K in ion beam nitrided austenitic stainless steel is investigated. Ar ion bombardment increases the N mobility in **depths far beyond the ion penetration depth (microns)**, resulting in an increased broadening of the N depth profile as a function of Ar flux. This effect cannot be explained by any established mechanism of radiation-enhanced diffusion. An explanation based on **qudon-enhanced mobility** is proposed



N penetration depth as a function of surface irradiating ion flux I for fixed ion fluence and different fluxes

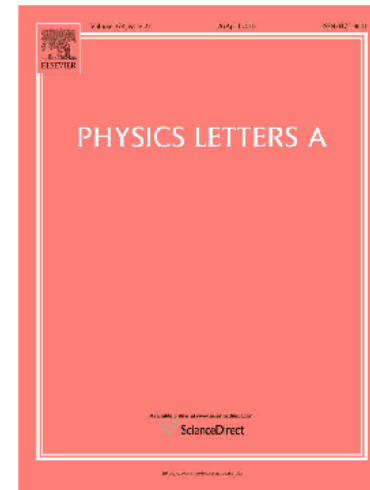
Long range effect of ion irradiation on diffusion

Li Zhang, Guangze Tang, Xinxin Ma, Physics Letters A 374 (2010) 2137–2139

Provided for non-commercial research and education use.
Not for reproduction, distribution or commercial use.

It was observed that low energy (500 eV) Ar ion irradiation significantly increased the substitutional Ni diffusion in quasi-single crystal Cu 0.5–1.5 mm away from the radiated surface.

The shorter the diffusion couple away from the radiated surface, the faster the Ni diffuses. It is suggested this effect is the result of an *effective energy migration decrease* by ion radiation induced DBs.



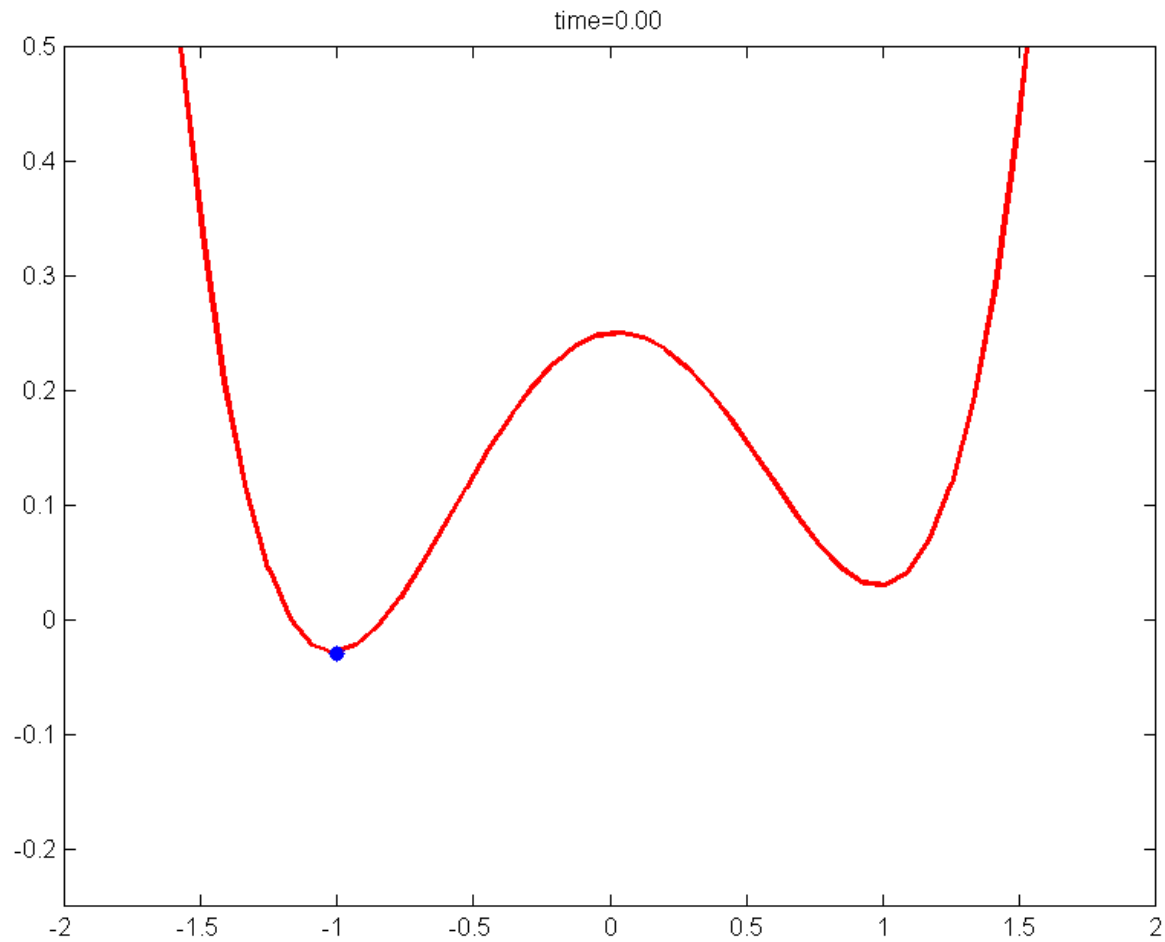
This article appeared in a journal published by Elsevier. The attached copy is furnished to the author for internal non-commercial research and education use, including for instruction at the authors institution and sharing with colleagues.

Other uses, including reproduction and distribution, or selling or licensing copies, or posting to personal, institutional or third party websites are prohibited.

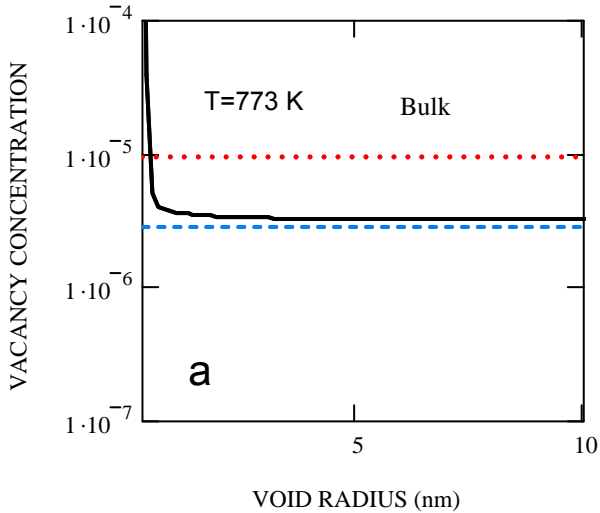
In most cases authors are permitted to post their version of the article (e.g. in Word or Text form) to their personal website or institutional repository. Authors requiring further information regarding Elsevier's archiving and manuscript policies are encouraged to visit:

<http://www.elsevier.com/copyright>

Quodon effect: random modulation



Dynamic Equilibrium vacancy concentration at voids, dislocations and free surfaces

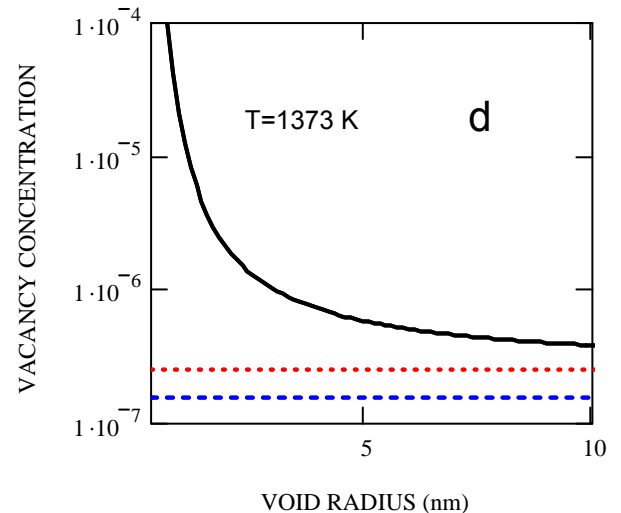
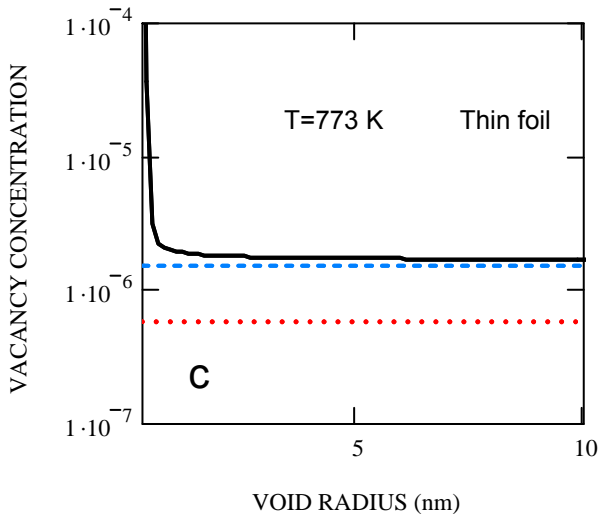
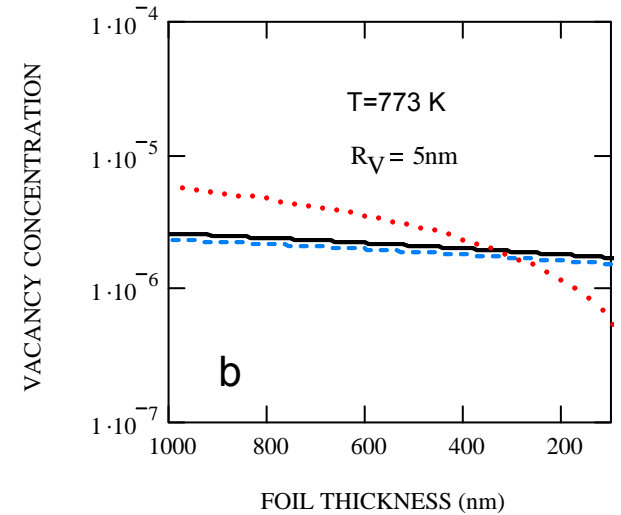


$$K = 8 \times 10^{-3} \text{ dpa/s}$$

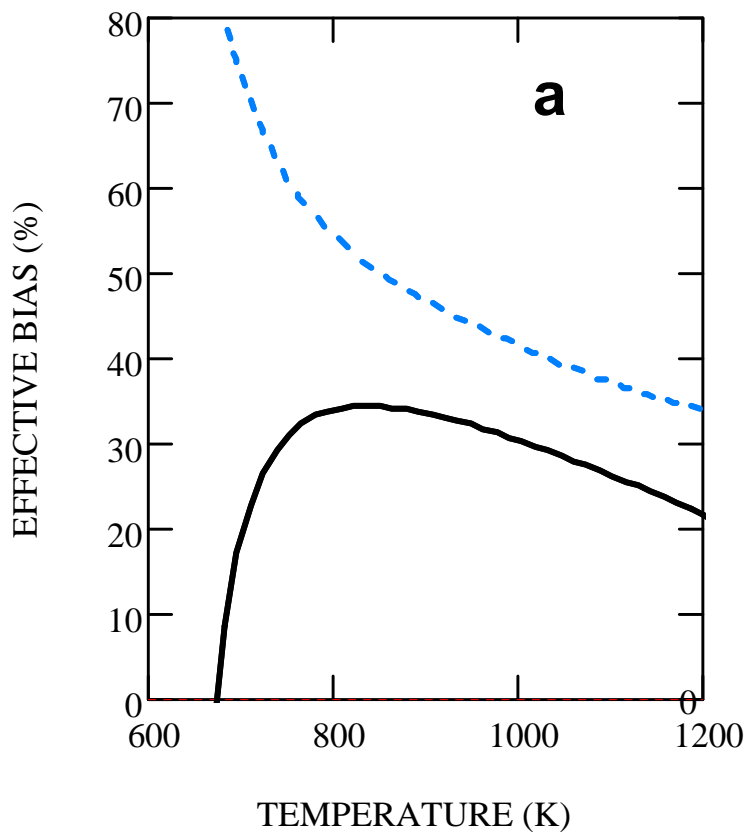
$$l_Q^0 = 5 \times 10^3 b$$

$$\Delta E_d = 0.5 \text{ eV}$$

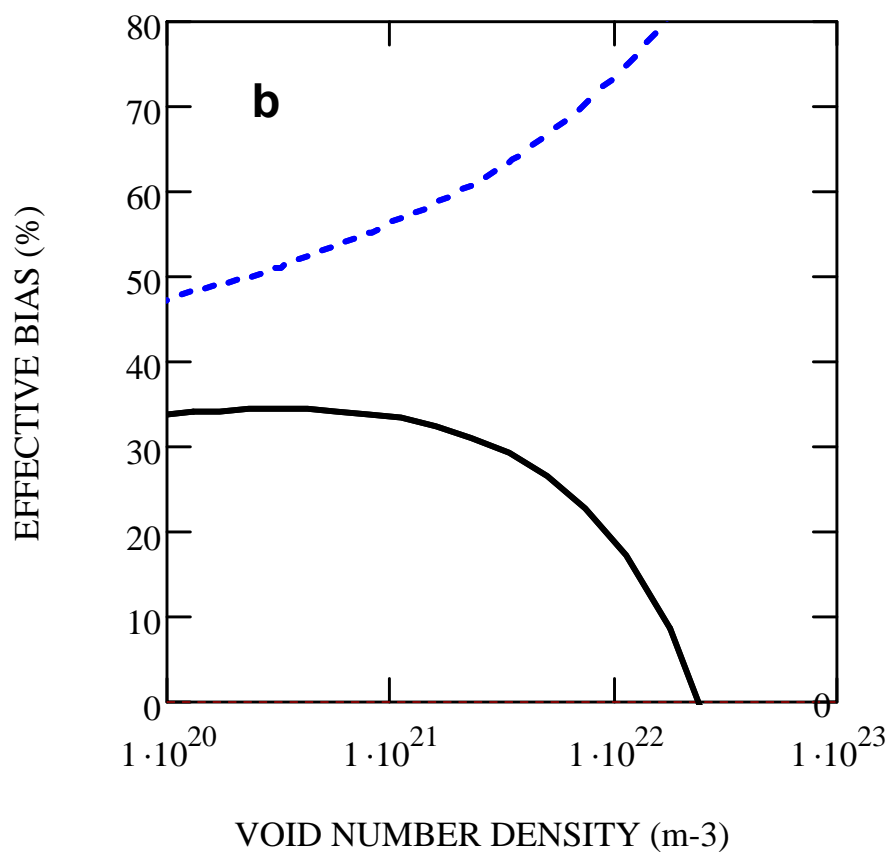
$$B_{em} \equiv \frac{k_v^2}{k_d^2} Z_v^V \frac{(D_v \bar{c}_v^{eq} - D_v c_v^{eq,V})}{D_i \bar{c}_i}$$



Evaluation of **effective bias** based on experimental data Makin et al. JNM (1980 -1985)

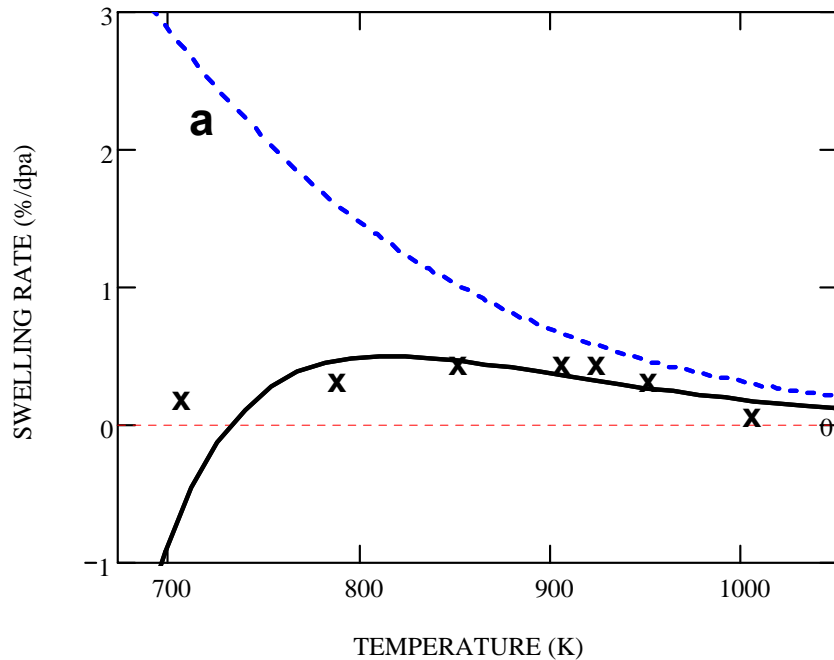


--- Early FP3D
— FP3D+EB

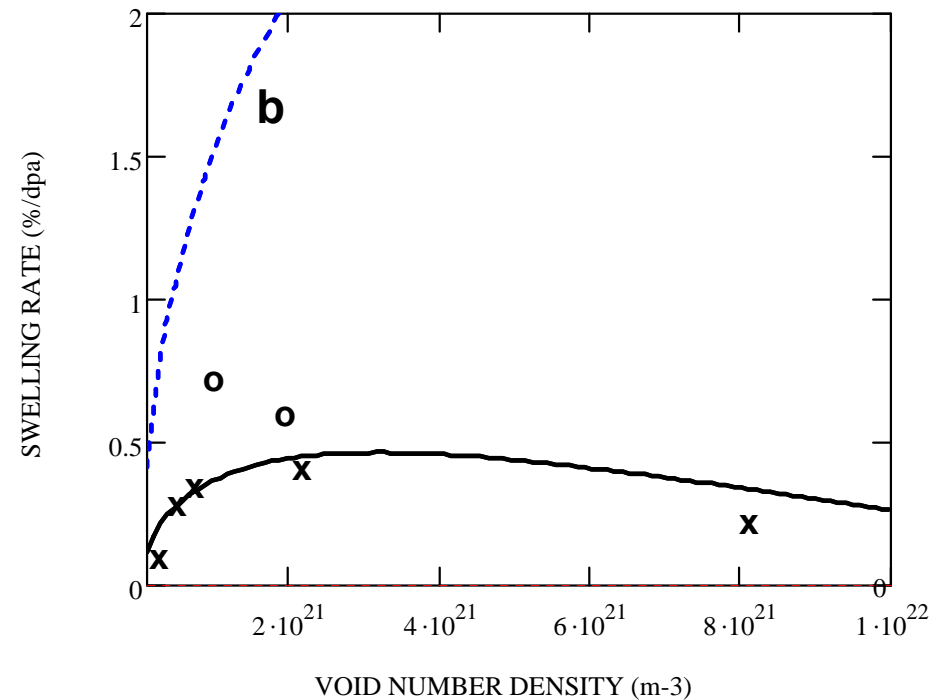


--- Early FP3D
— FP3D+EB

Evaluation of swelling rate in new FP3DM and comparison with experimental data Makin et al. JNM (1980 -1985)



--- Early FP3DM
 — FP3DM+EB



--- Early FP3D
 — FP3D+EB

Swelling rate calculated as a function of temperature and the void number density. Experimental data for austenitic steel (a) and for a pure Fe-Ni-Cr alloy (b), where **x** and **o** represent residual gas and 10 appm pre-injected helium

Bakuriani, Georgia



HISTORY

30 years ago

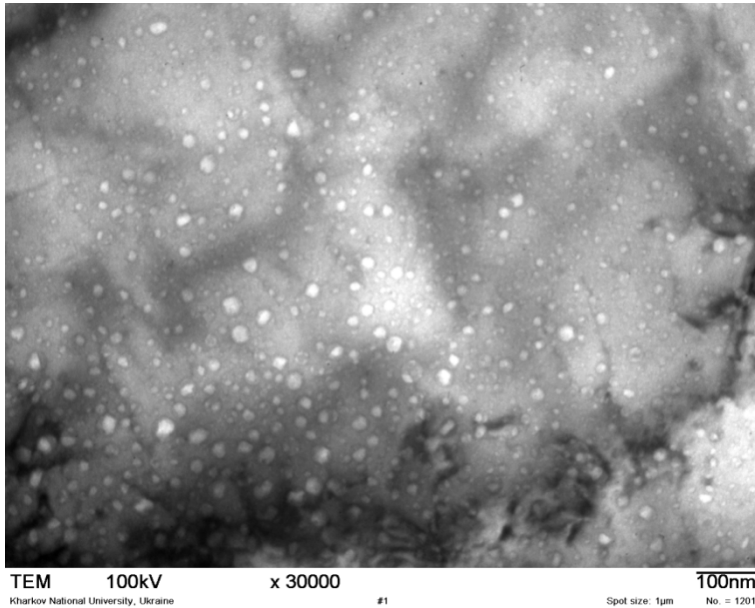
“For many years already we study the void swelling in reactor materials, but to solve the problem one should know how the void shrink rather than grow...”

Ilya Naskidashvilly, Winter School, Bakuriani, Georgia 1980

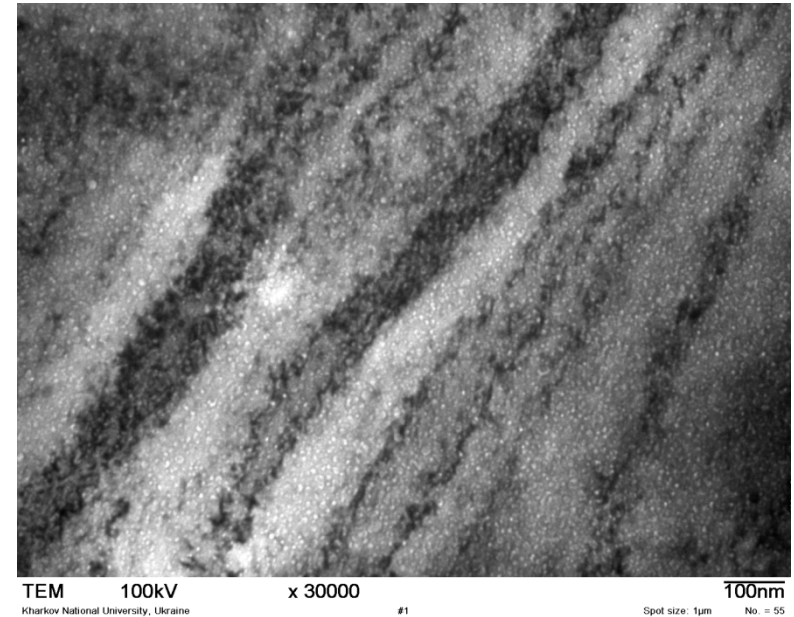
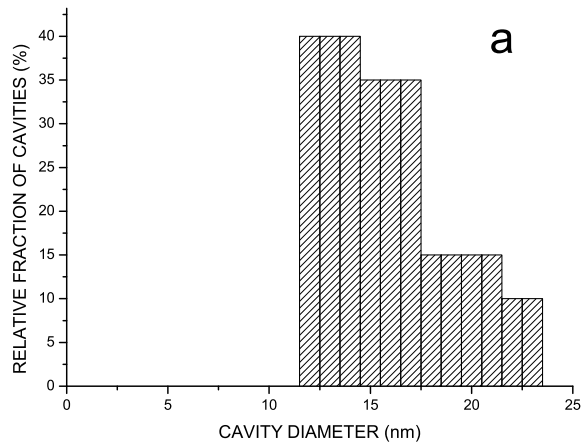
29 years later...



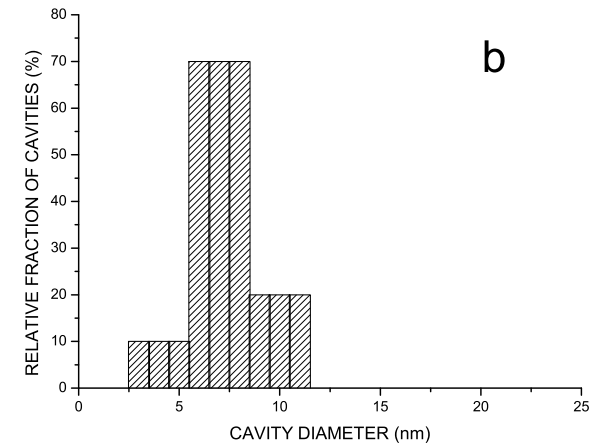
Radiation-induced “annealing” of voids under 30 keV proton irradiation (Dubinko, Guglya et al, 2009)



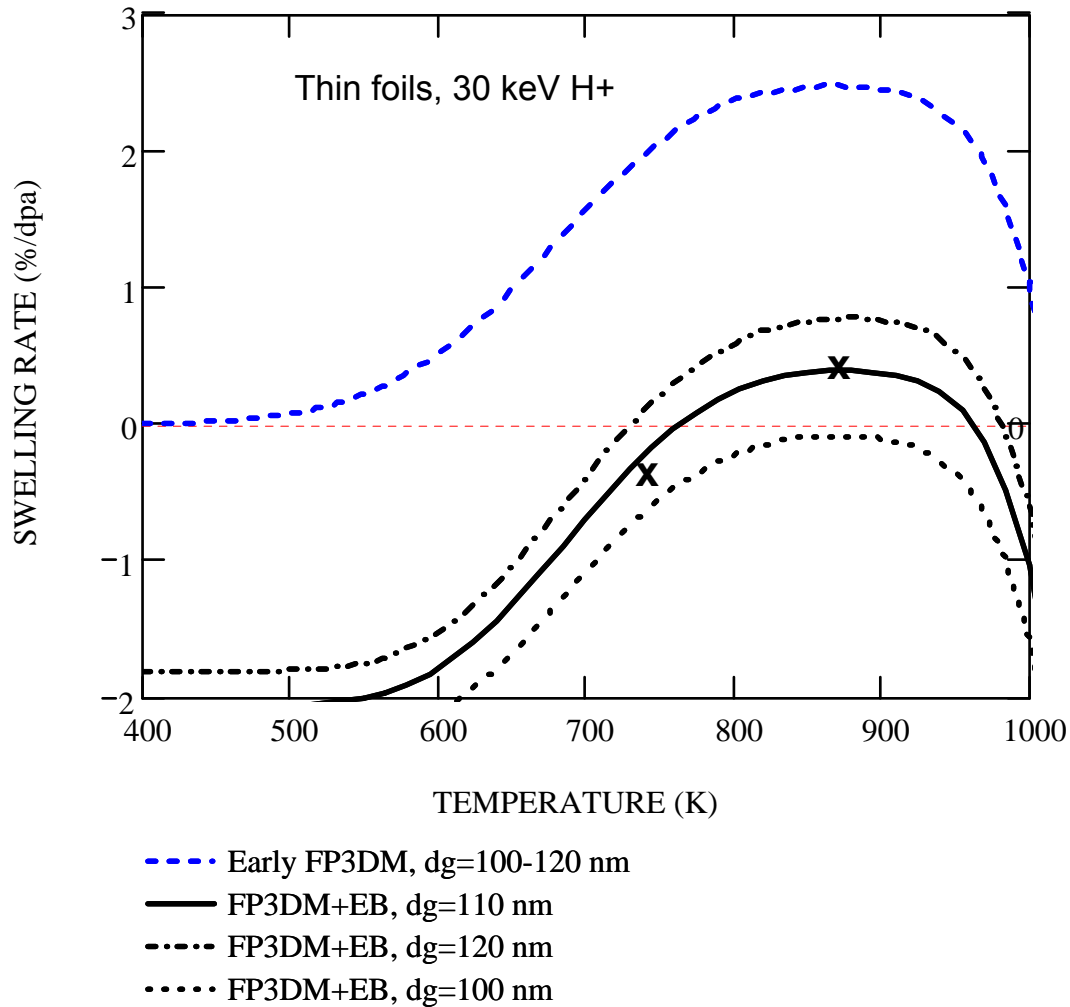
$10P^{18P}$ ion/cm P^{2P} HP^{+P} (30 keV) ~ 6 dpa at 873 K



6 dpa at 873 K + 12 dpa at 723 K



Theory vs. experimental data



Temperature dependence of swelling rate in nickel foils irradiated with 30 keV protons vs. experimental data:

$$K = 6 \times 10^{-4} \text{ dpa/s}, \quad \bar{R}_v = 10 \text{ nm}, \quad N_v = 10^{22} \text{ m}^{-3}, \quad \rho_d = 2 \times 10^{14} \text{ m}^{-2}, \quad l_Q^0 = 5 \times 10^3 \text{ b}, \quad \Delta E_d = 0.5 \text{ eV};$$

Wolfer Response

I took a close look at the manuscript by Dubinko et al, and I am in full agreement with their assessment of the production bias and its failure to explain actual experimental results. We also had reached this conclusion and stated our objections in Ref.5 quoted by Dubinko.

What impressed me the most, however, is the new mechanism of radiation-enhanced vacancy emission from dislocations, voids and grain boundaries. The theoretical treatment of this new effect is very sound, although to some degree approximative. The inclusion of it into the classical rate theory is handled correctly, and applying it to the experiments discussed in the paper provides then compelling validation of the new rate theory. I recommend that the paper be published. However, I did not take enough time to look for typos or list cases of awkward English; this, I assume, will be taken care of by the editors. But I am willing to serve as a referee.

With best regards,

Bill Wolfer

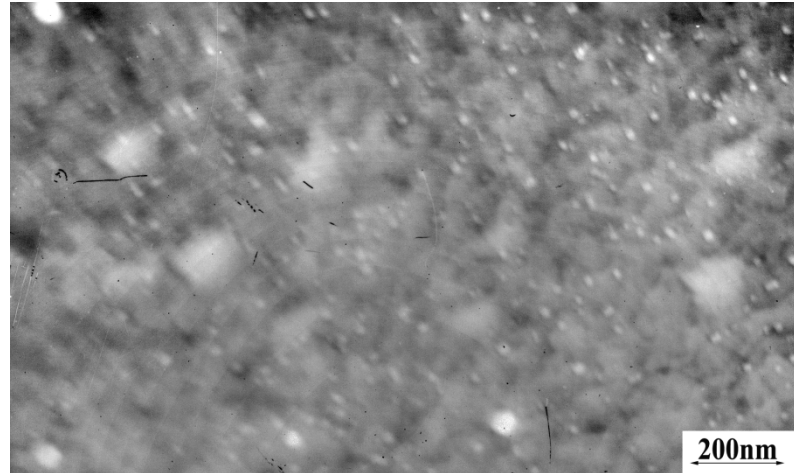
Irradiation of nickel with chromium ions

V.I. Dubinko, A.G. Guglya, E. Melnichenko, R. Vasilenko, EMRS 2008,
Journal of Nuclear Materials, 385 (2009) 228-230

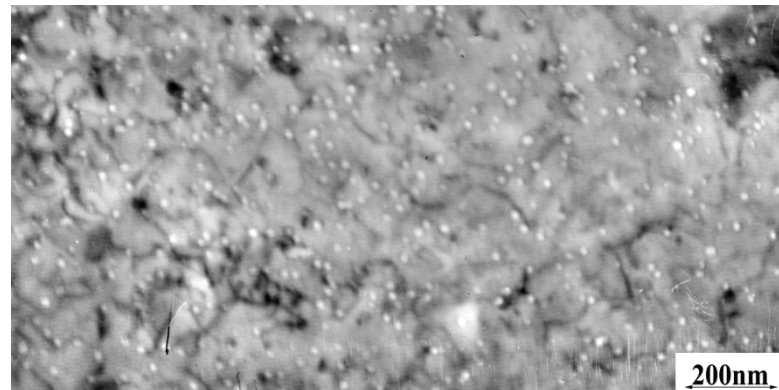
$\text{Cr}^{3+} \rightarrow \text{Ni}$ (600°C, ~25 dpa)



$\text{Cr}^{3+} \rightarrow \text{Ni}$ (600°C, ~25 dpa) + $\text{Cr}^{3+} \rightarrow \text{Ni}$ (525°C, ~25 dpa)



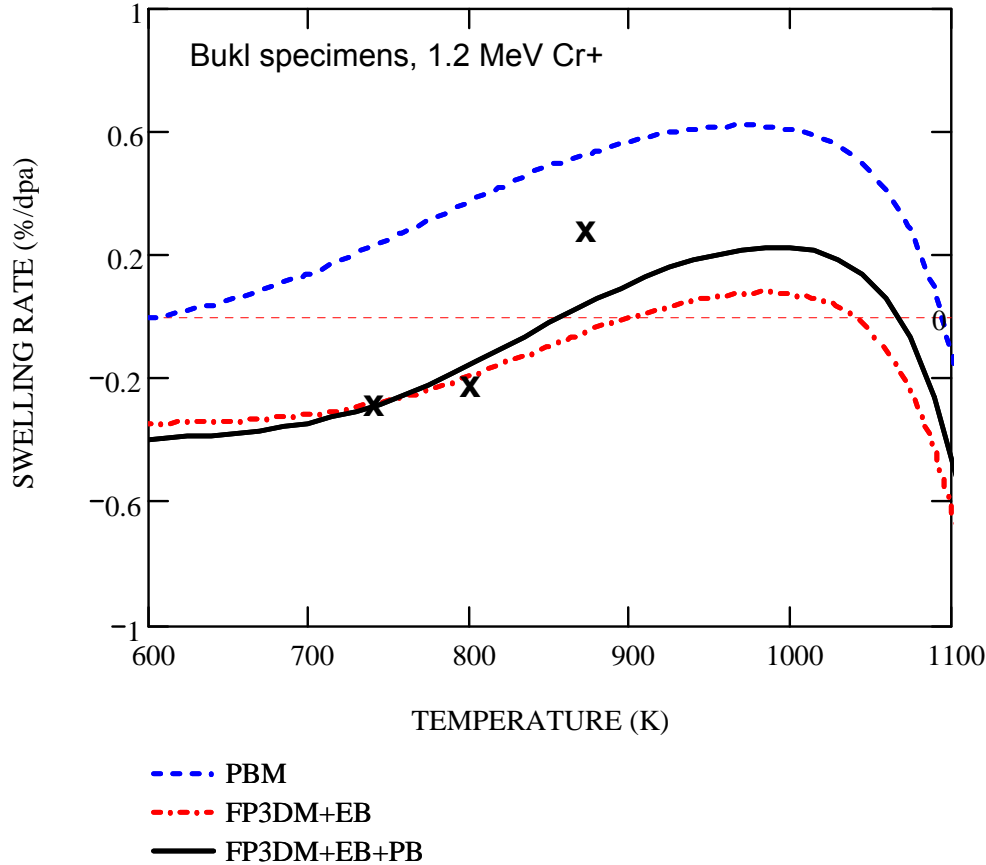
$\text{Cr}^{3+} \rightarrow \text{Ni}$ (600°C, ~25 dpa) + $\text{Cr}^{3+} \rightarrow \text{Ni}$ (450°C, ~25 dpa)



ION FLUENCE 10^{21} ions/m²

DOSE RATE $K = 7 \times 10^{-3} \text{ s}^{-1}$

Theory vs. experimental data



$$\frac{dS}{dt} = D_i \bar{c}_i \frac{k_{Vv}^2 k_{dv}^2}{k_v^2} B_{tot}$$

$$B_{tot} \equiv B_{ab} - B_{em} + B_p$$

$$B_{em} \equiv \frac{k_v^2}{k_d^2} Z_v^V \frac{(D_v \bar{c}_v^{eq} - D_v c_v^{eq,V})}{D_i \bar{c}_i}$$

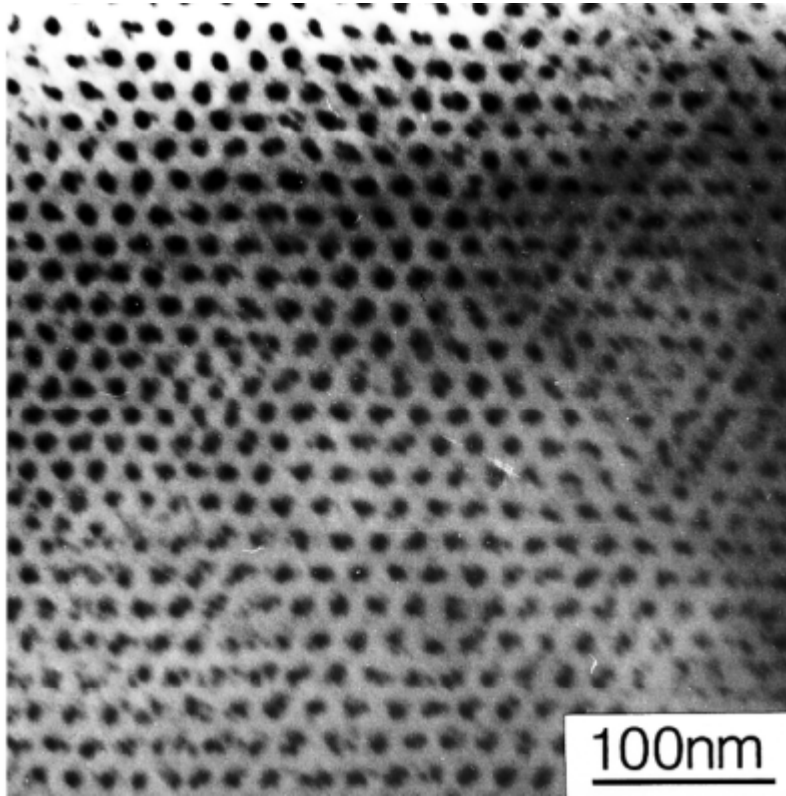
$$B_p \equiv \frac{\varepsilon_i k_{eff} K}{k_{dv}^2 D_i \bar{c}_i} \left(1 - \frac{k_v^2 \bar{R}_V}{8l_g} \right)$$

Temperature dependence of swelling rate in nickel bulk samples irradiated with 1.2 MeV Cr ions vs. experimental data: $K = 7 \times 10^{-3}$ dpa/s, $\bar{R}_V = 20$ nm, $N_V = 10^{21} m^{-3}$, $\rho_d = 2 \times 10^{14} m^{-2}$.

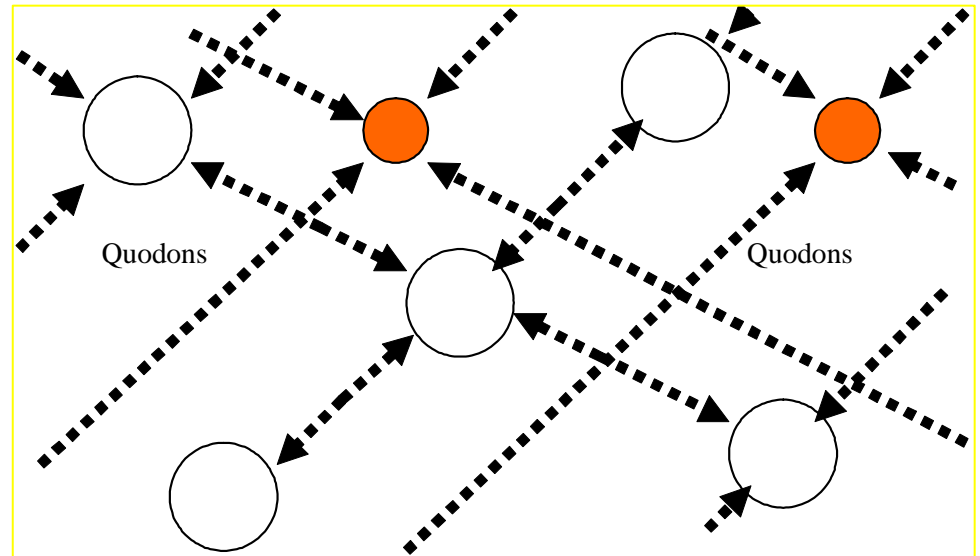
$l_Q^0 = 5 \times 10^3 b$, $\Delta E_d = 0.5$ eV – EB parameters

$k_{eff} = 0.1$, $\varepsilon_i = 0.2$ – PB parameters

Swelling saturation and void ordering

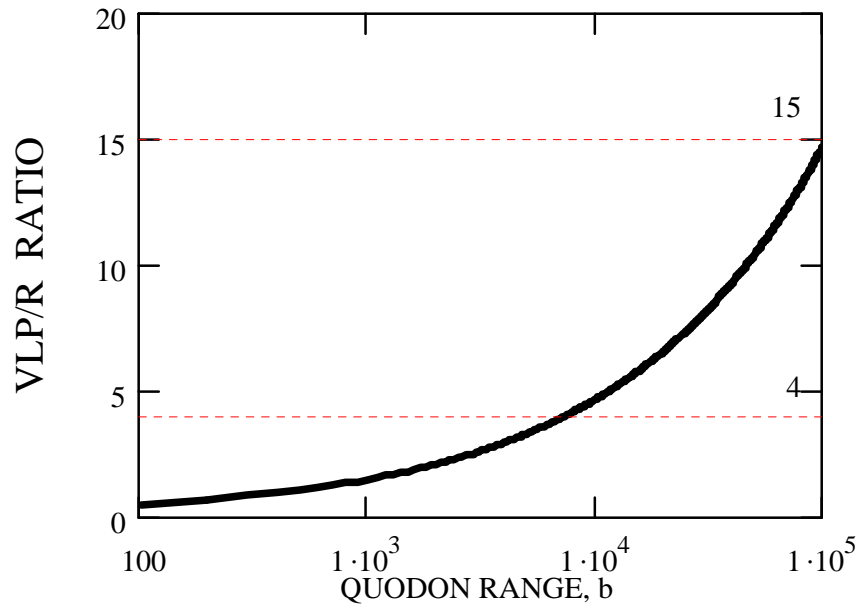


Micrographs of bcc void lattices following ion irradiation in molybdenum, (111) projection [J.H. Evans, in *Patterns, Defects and Materials Instabilities*, 1990].



Dissolution of a void in the “interstitial” position due to the absorption of quodons coming from larger distances as compared to “regular” voids [V. Dubinko, *Nuclear Inst. and Methods in Physics Research*, 2009]

Void lattice parameters



Dependence of the VLP/R ratio on the quodon range:
The markers show the experimentally observed range of VLP/R ratio values in different materials

$$a_{VL}/\bar{R} \approx (\alpha_{iv}^*)^{-2/3} (k_D^2 \delta_D)^{1/6} (K_Q l_Q b / K_{FP})^{1/2}$$

Long range effects in metals

Materials modification by low-energy ion irradiation

I. V. Tereshko, V. I. Khodyrev, E. A. Lipsky, A. V. Goncharenya and A. M. Tereshko

Nuclear Instruments and Methods in Physics Research Section B: Beam Interactions with Materials and Atoms, 127-128 (1997) 861-864

The modification of materials subjected to the bombardment with low-energy ions was investigated. The increase of dislocation density in metal samples was **observed up to a depth of 10 mm** from the irradiated surface. It is described as a “long-range effect”. The low-energy ion irradiation leads to the change of physical and mechanical properties of irradiated materials. This is, actually, a bulk modification. To explain this modification of materials the authors suggest a hypothesis based on the **idea of nonlinear oscillations excitations in crystals** which lead to active self-organizing processes in the ion subsystem.

Long range effects in metals

On depth of the zone of modification of properties (hardening) of materials under irradiation at $t < 100$ °c with low-energy plasma of the glow discharge

Y.V. Kunchenko, V.V. Kunchenko, G.N. Kartmazov

NSC Kharkov Institute of Physics and Technology, Kharkov, Ukraine

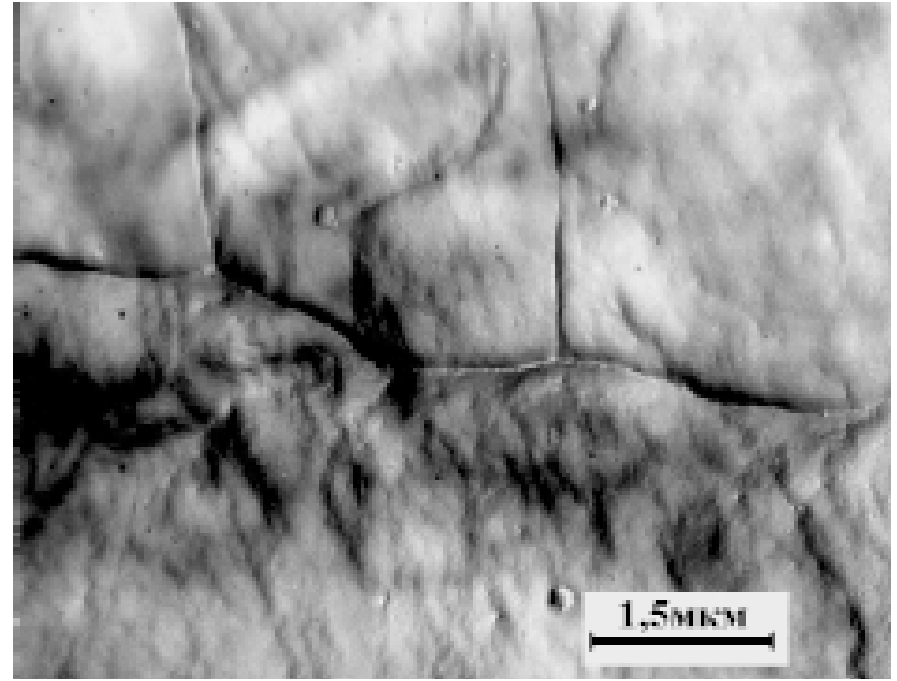
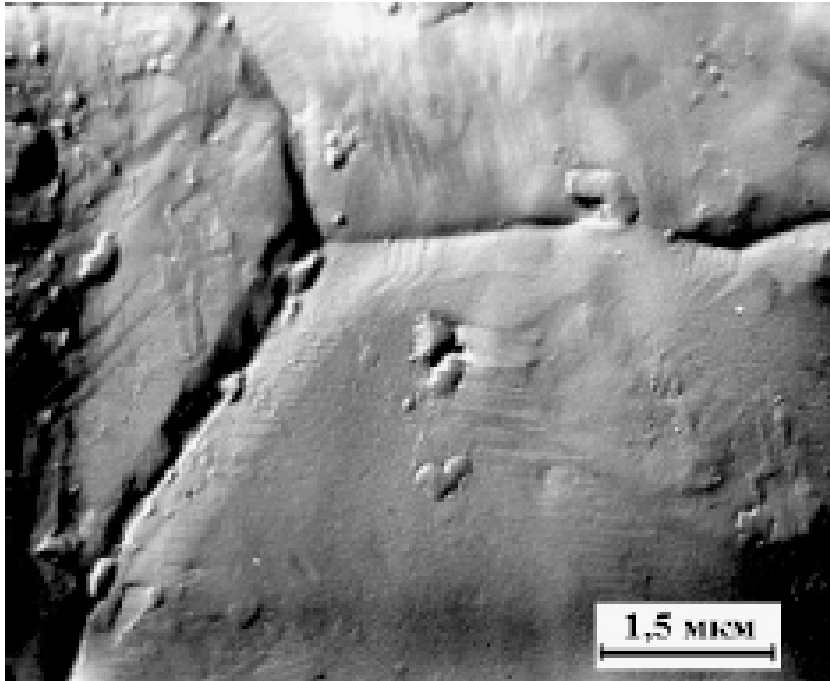
ФІП ФІП PSE, 2009, т. 7, № 1-2, vol. 7, No. 1-2 (in Russian)

The macroscopical scale the modified (strengthened) zone is established on the basis of results of measurements of distribution of microhardness on depth (up to 2,5 mm) initial deformed, annealed (600 °C, 2,5 hours) and irradiated with low energy plasma of the glow discharge at $T < 100$ °C samples alpha-Fe, and two-fold increase of relative erosive stability (resistance) of the irradiated samples of steel HVG at cavitation influence of water at the *back side* of a sample, which thickness was 4 mm. Features of changes of a microstructure of the irradiated coarse-grained samples of alpha-Fe and the fact of hardening of the back (not irradiated) surface of a sample of steel confirm the wave nature of the mechanism of long-range action, transport of energy of an elastic wave at macrodistances from the irradiated surface.

On depth of the zone of modification of properties (hardening) of materials under irradiation at $t < 100$ °c with low-energy plasma of the glow discharge

Y.V. Kunchenko, V.V. Kunchenko, G.N. Kartmazov

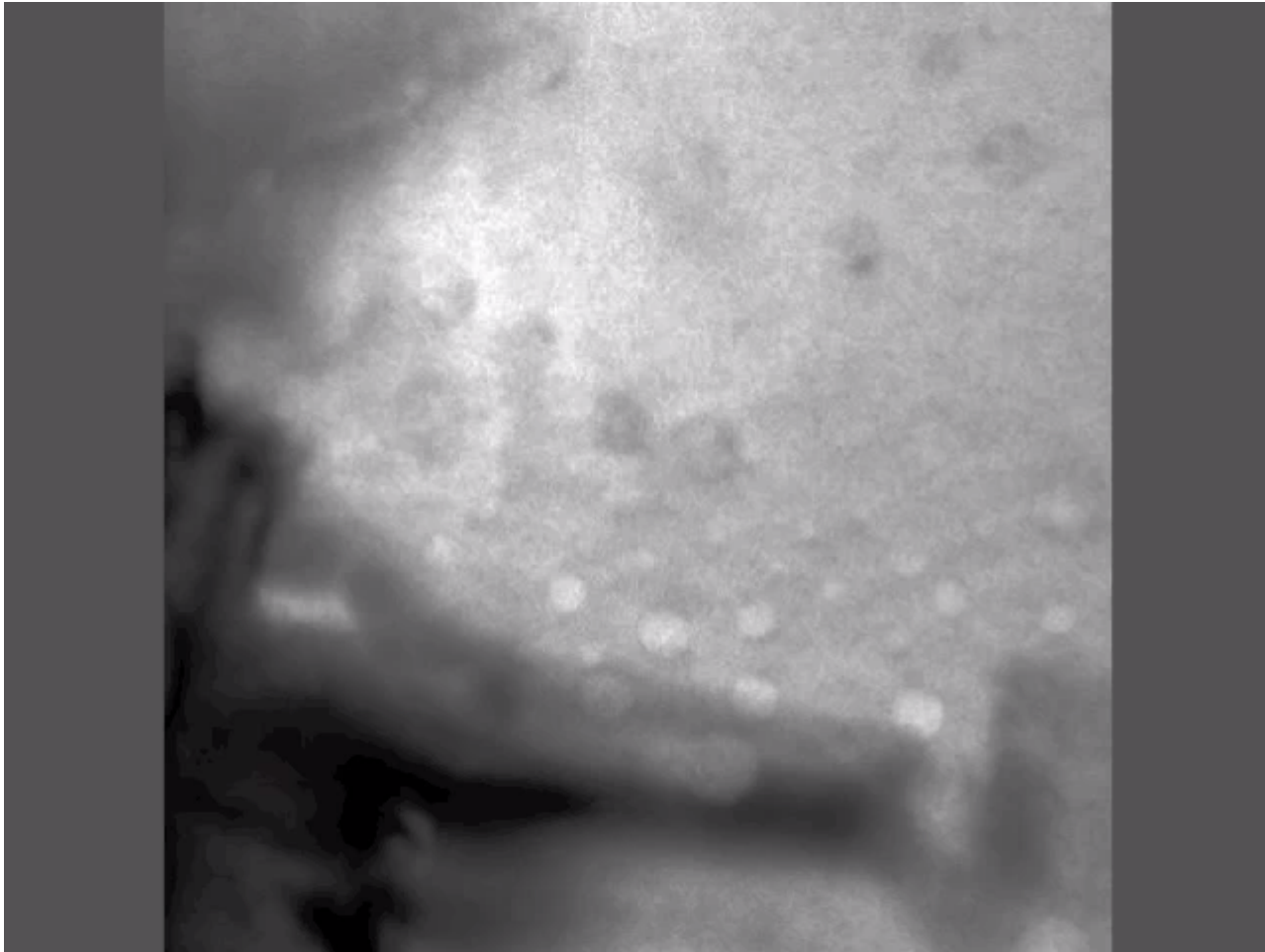
NSC Kharkov Institute of Physics and Technology, Kharkov, Ukraine



Microstructure of alpha-Fe in the annealed state before irradiation (left) and after irradiation with low energy plasma of the glow discharge (right). Formation of dense dislocation networks around grain boundaries can be seen far away from the irradiated surface

Sub-threshold electron irradiation

Salford, UK, 2011



SUMMARY

- The rate theory modified with account of quodon-induced reactions has been applied for description of the radiation-induced **growth** and **annealing** of voids.
- The best agreement with experiment shows the model that takes into account all three constituents of swelling, based on the absorption, emission and production biases.

The quodon **propagation range** in different metals deduced from the comparison between the theory and experiment are in the **micron range**, which is consistent with an **typical grain size**.

- In order to forecast the behavior of nuclear materials one has to know the **generation rate** of quodons and their **propagation range** in different crystal structures as the functions of **impurity atom concentration and type**. The latter factor seems to be of a primary technological importance since it offers a new insight on **design of radiation-resistant materials**.



1st International Workshop Nonlinear Effects in Materials under Irradiation (NEMI 2012)

12-17 February, 2012. Pretoria, South Africa



Scope The workshop is devoted to physical phenomena and effects in materials subjected to irradiation. Radiation environment gives rise to many nonlinear interactions between electron and atomic subsystems, lattice solitons, crystals defects etc. The main attention will be focused on three interconnected aspects:

- (i) A detailed discussion of the physical nature of nonlinear phenomena and effects.
- (ii) Theoretical models of nonlinear phenomena and possible universal laws they predict.
- (iii) Application of new ideas, methods and results of

mathematical physics and computational mathematics in the radiation material science.

Organizing Committee

Pavel Selyshchev
Chris Theron
Sergey Rakityanskiy
Vladimir Skuratov

Programme Committee

Vladimir Dubinko
Johan Malherbe
Vladimir Sugakov
Shenyang Hu

Nomination of Dr Dubinko for the 2012 Robert Cahn Award from Foreign Scientists:

Organization: Lawrence Livermore
National Laboratory
Person: **Prof. Craig Smith**
Address: Livermore, California 94551
United States of America

Organization: University of Huddersfield
Person: **Prof. Steve Donnelly**
Address: Queensgate, Huddersfield
HD1 3DH, United Kingdom

Organization: Heriot-Watt University
Person: **Prof. Mike Russell**
Address: Edinburgh, EH14 4AS,
United Kingdom

Organization: Seville University
Person: **Prof. Juan Archilla**
Address: Seville, Andalusia E-41011,
Spain

Organization: University of Pretoria
Person: **Prof. Pavel Selyshchev**
Address: Hatfield 0028, Private bag X20
South Africa

Organization: Pacific Northwest National
Laboratory
Person: **Dr. Shenyang Hu**
Address: Richland, , WA 99352,
United States of America

Organization: Atomic Energy Canada
Limited
Person: **Dr. Malcolm Griffiths**
Address: Chalk River, Ontario,
K0J 1J0, Canada

Organization: AERE Harwell
Person: **Dr. John Evans**
Address: 27, Cleavelands, Abingdon
OX142EQ, United Kingdom

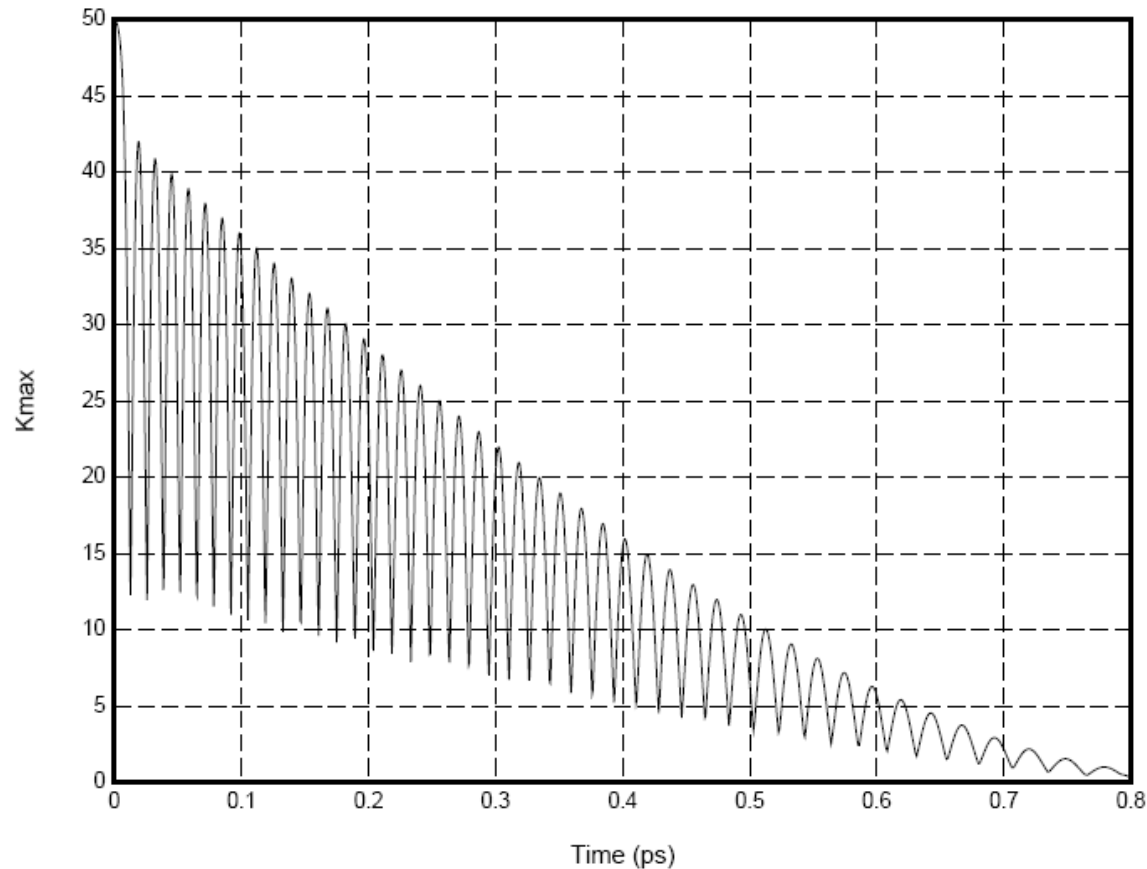
Organization: Max-Planck-Institut fuer
Physik komplexer Systeme
Person: **Dr. Sergei Flach**
Address: Noethnitzer Str. 38, D-01187
Dresden, Germany

Organization: Institute of Metallophysics
NAS of Ukraine
Person: **Prof. Sergij Kotrechko**
Address: Vernadsky Ave, 36,
Kyiv, Ukraine,

**THANK YOU
FOR
YOUR ATTENTION!**

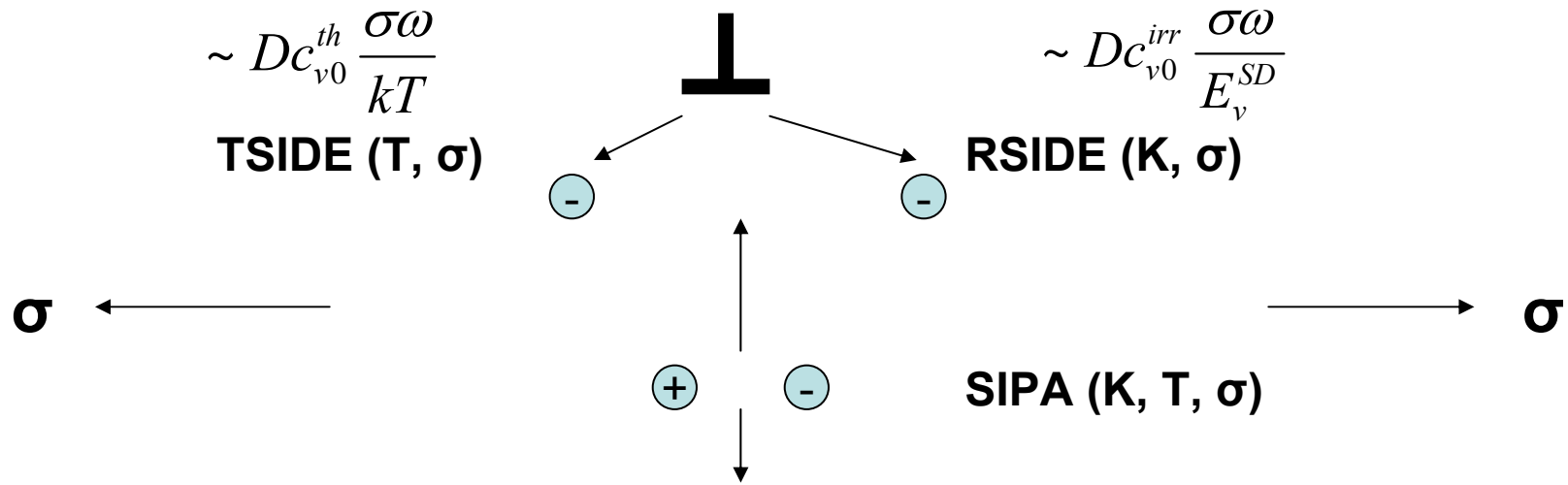
Outstanding problem:

How to observe quodons in conventional MD ?



The energy relaxation simulations in Cu at $T = 1$ K,
Lazarev, Dubinko, 2003

Irradiation creep



$$D_v c_{v0}^{th} = D_{v0} \exp\left\{-\frac{E_v^{SD}}{kT}\right\}$$

$$Dc_{v0}^{irr} \approx K \left(\frac{E_d}{E_v^{SD}}\right)^n bl_F^0$$

Irradiation creep due to **radiation** and **stress**-induced difference in vacancy **emission** from dislocations (**RSIDE**)

$$\dot{\epsilon}_{SIDE} = \dot{\epsilon}_{TSIDE} + \dot{\epsilon}_{RSIDE}$$

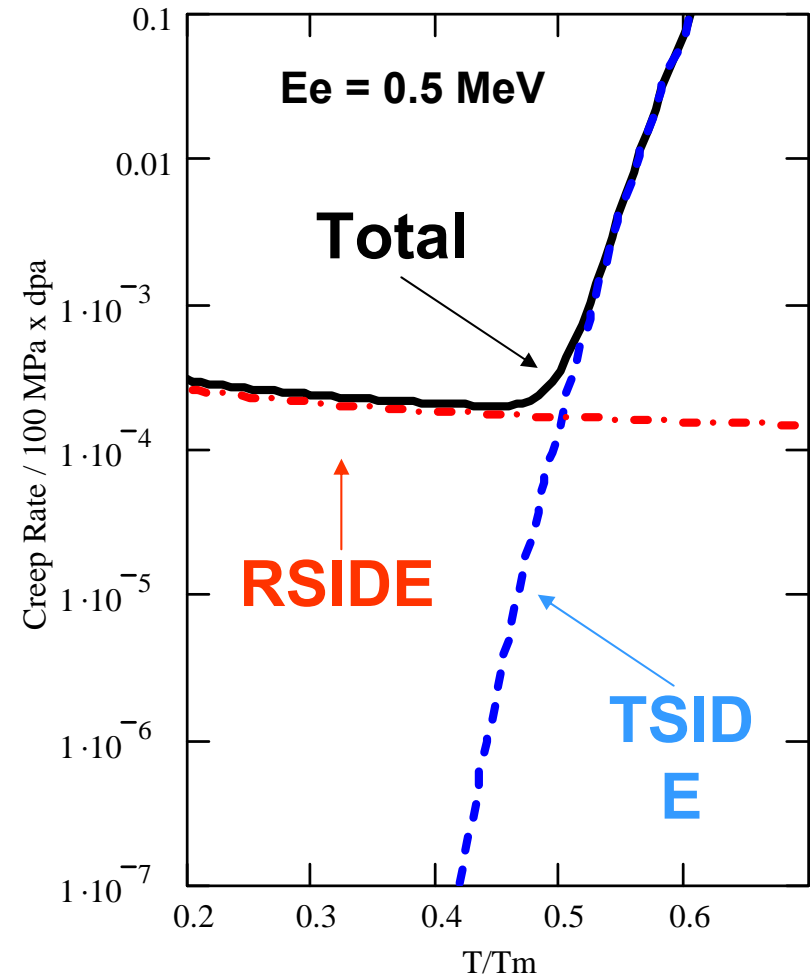
Thermal creep rate:

$$\dot{\epsilon}_{TSIDE} \approx \rho_d D_v c_v^{th} \frac{\sigma \omega}{k_B T}$$

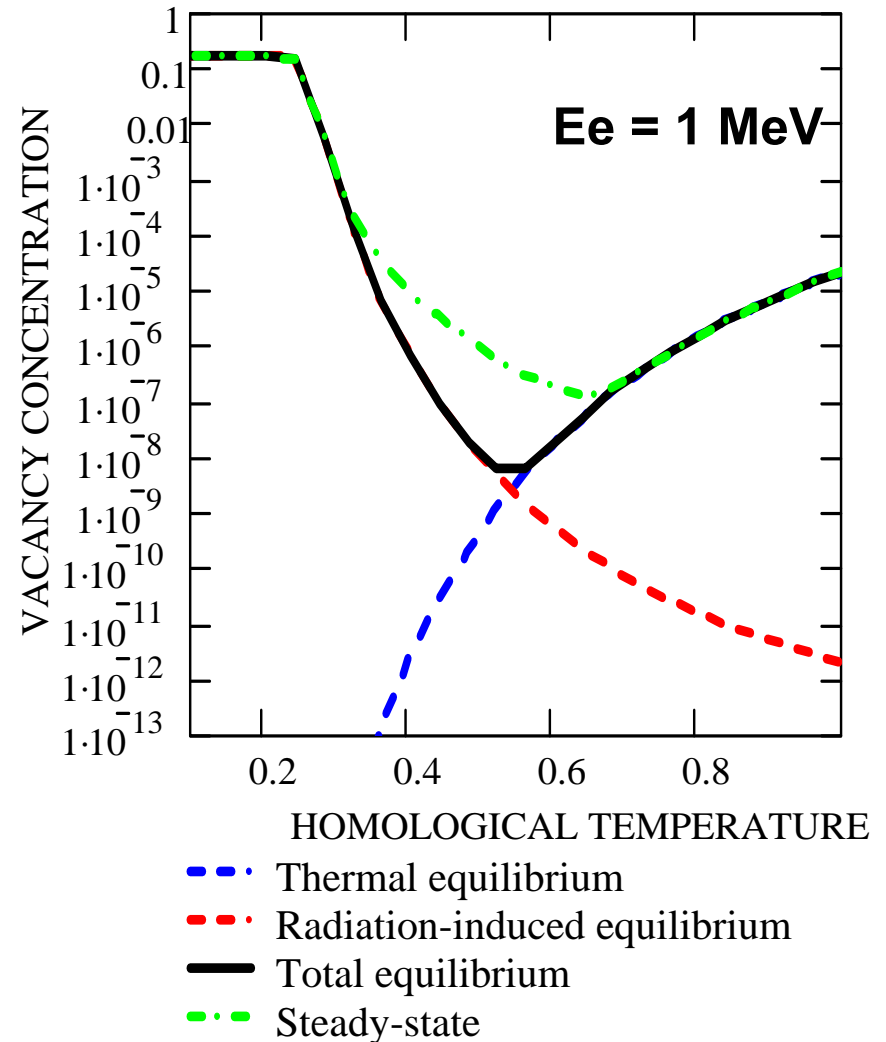
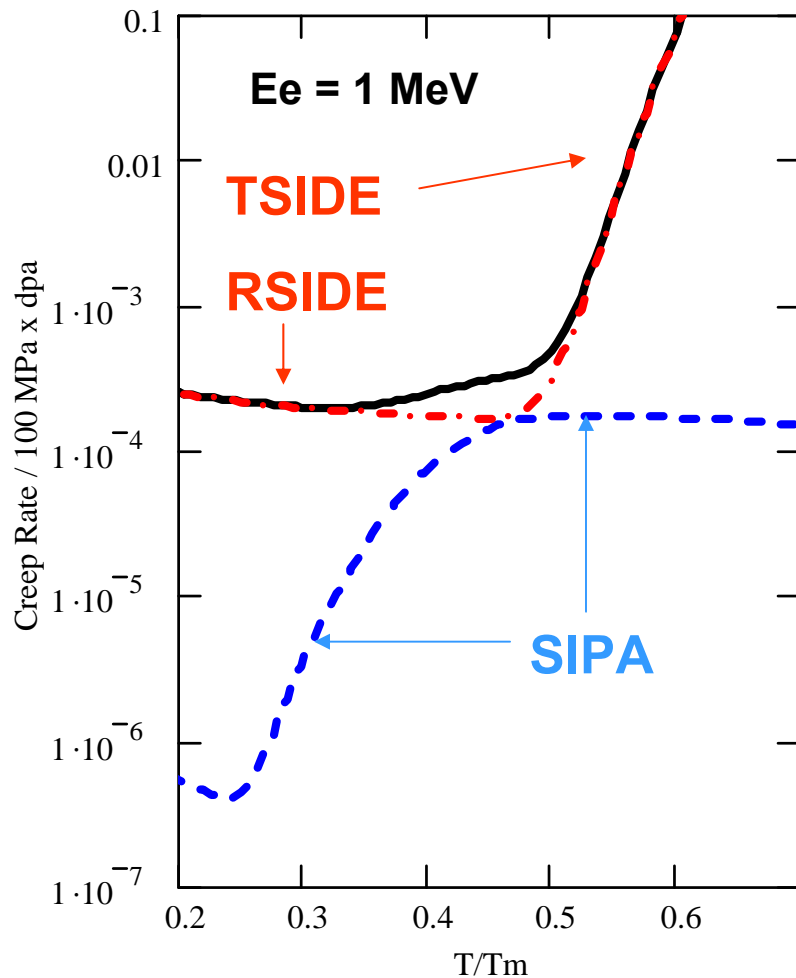
Irradiation creep rate:

$$\dot{\epsilon}_{RSIDE} \approx \rho_d D_v c_v^{irr} \frac{\sigma \omega}{E_v^f + E_v^m}$$

Sub-threshold irradiation



Comparison between the SIPA and SIDE creep rates

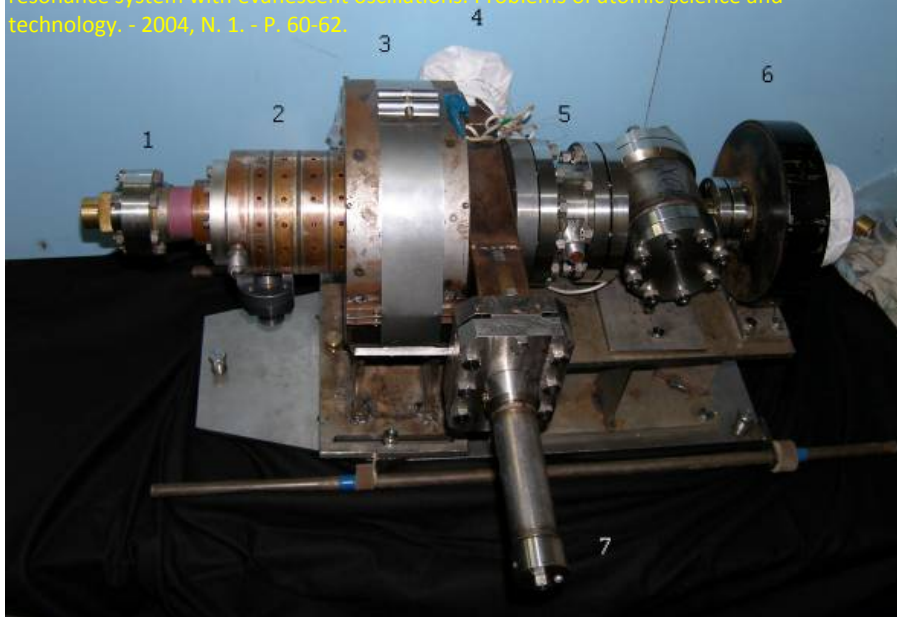


ELECTRON-PLASTIC EFFECT

Experimental investigation of the electron-plastic effect under electron irradiation

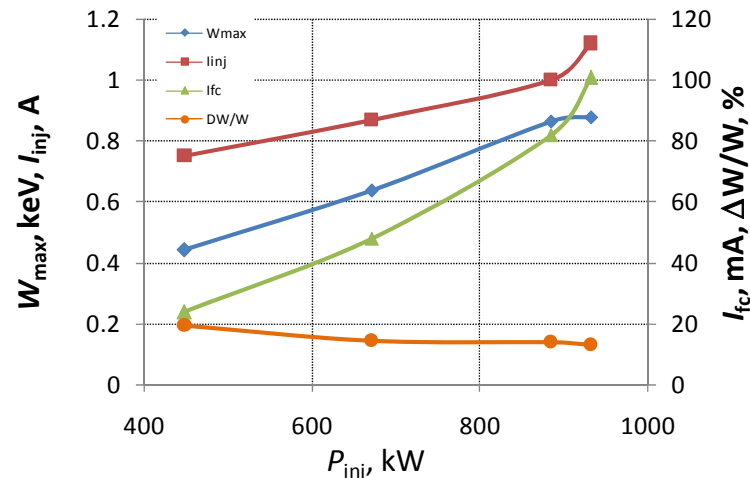
Kushnir, Lebedev et al, NSC KIPT, 2008

* M.I. Ayzatsky, E.Z. Bifer, N.G. Golovko et al. Electron injector based on resonance system with evanescent oscillations. Problems of atomic science and technology. - 2004, N. 1. - P. 60-62.



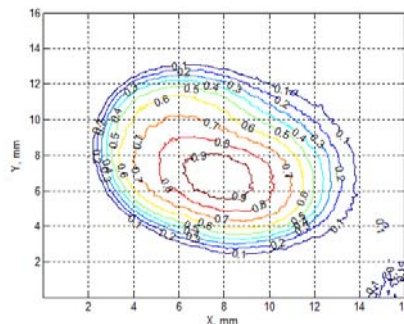
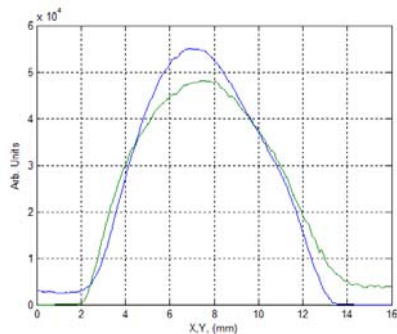
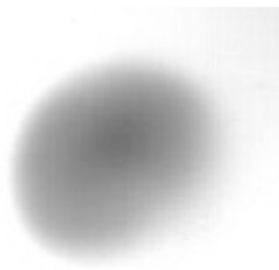
Инжектор в сборе: 1 – катодный узел электронной пушки, 2 – группирователь, 3 – соленоид, 4 – подводящий волновод, 5 – датчик тока пучка, 6 – магнитная линза, 7 – механизм перемещения короткозамкнутого поршня

Диапазон основных параметров пучка в зависимости от мощности СВЧ питания



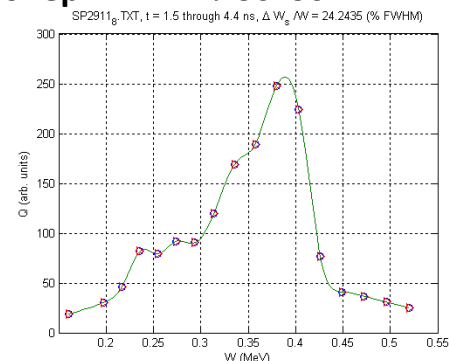
W_{max} – энергия электронов на выходе источника,
 I_{inj} – ток пучка электронов на выходе источника,
 I_{fc} – ток пучка электронов в плоскости мишени,
 $\Delta W/W$ – ширина энергетического спектра

Отпечаток пучка в плоскости мишени



$\Delta X = 7.9492$ mm, $\Delta Y = 7.0343$ mm (на уровне половинной интенсивности)

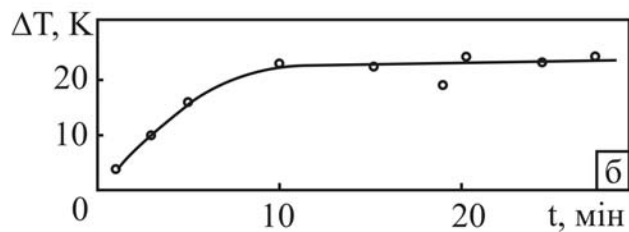
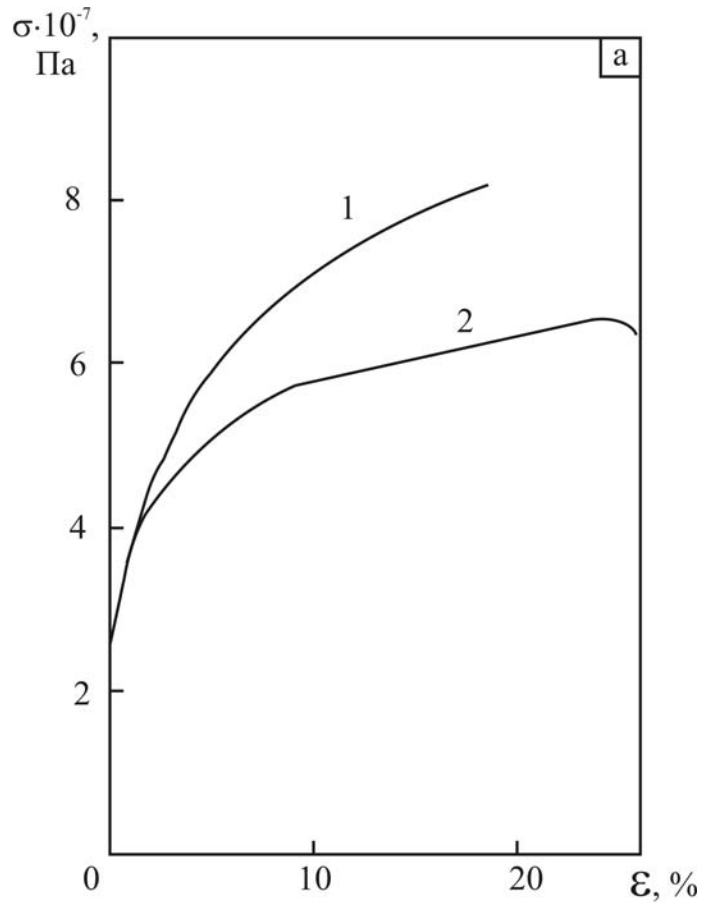
Распределение электронов по энергиям в плоскости мишени



$W_{max} = 390$ keV, $\Delta W/W = 24\%$ (FWHM)

Experimental investigation of the electron-plastic effect under electron irradiation

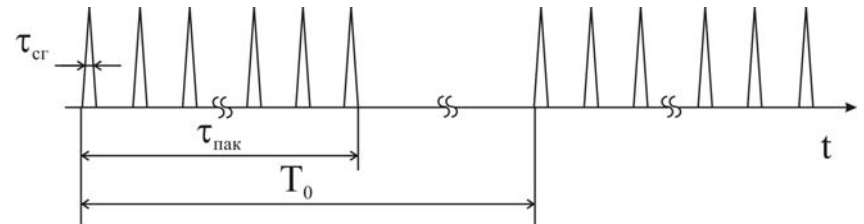
Dubinko, Lebedev, Kushnir et al, NSC KIPT, 2008



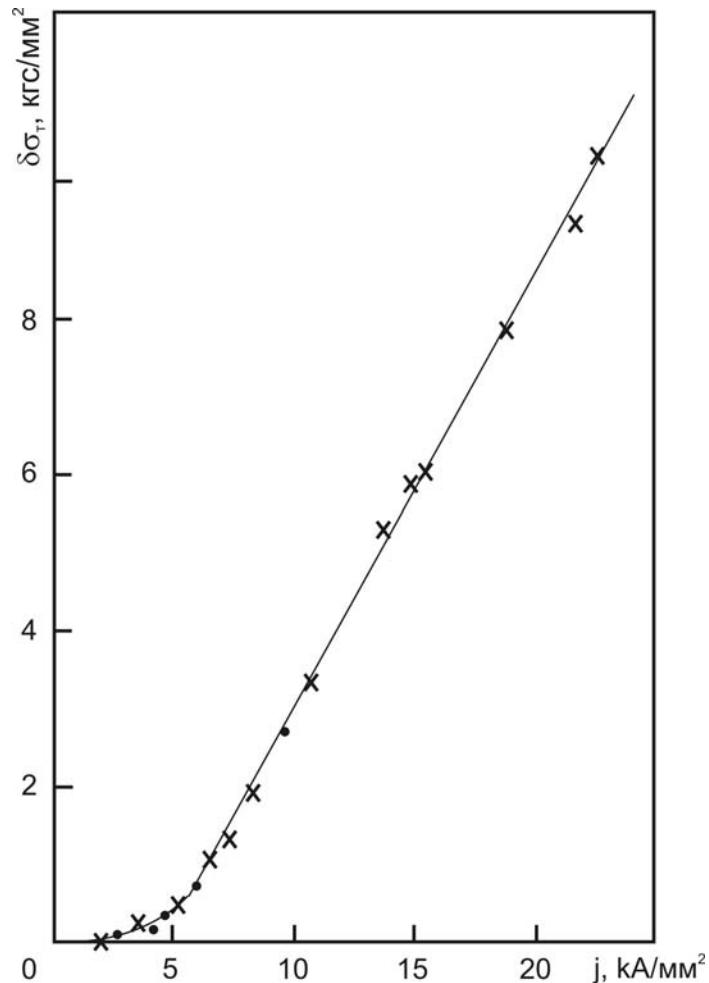
Deformation hardening of aluminum samples (a) without irradiation (1) and under irradiation with electrons (2); (b) Temperature evolution under irradiation

$$T_{\text{пак}} = (1-3) \times 10^{-6} \text{ s}, \quad w_{\text{пак}} = 50 \text{ Hz},$$

$$\varphi_e = 5 \cdot 10^{13} \text{ cm}^{-2} \text{ s}^{-1}$$



Experimental investigation of the electron-plastic effect under electric current

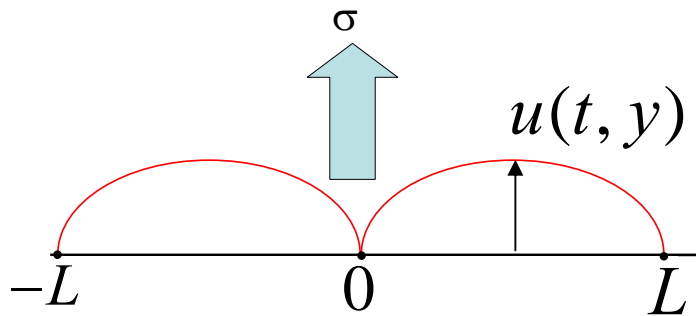


EPE dependence on the electric current density in Cu (99.5%) at 300 K and the strain rate is 2.7×10^{-4} s
[Lebedev et al, Kharkov National University, 2008]

The linear dependence can not be explained by Joule heating of the sample

String model of the dislocation segment oscillations

A.I. Landau, Yu.I. Gofman, 1974



$$M \frac{\partial^2 u}{\partial t^2} + B \frac{\partial u}{\partial t} - C \frac{\partial^2 u}{\partial y^2} = b\sigma + f(t)$$

$$U(x) = \begin{cases} \zeta x^2, & |x| \leq x_{kp} \\ 0, & |x| > x_{kp} \end{cases} \quad \zeta x_{kp}^2 = U_0$$

$$u'_y(0, t) = \kappa u(0, t) \quad -u'_y(L, t) = \kappa u(L, t) \quad \kappa = \frac{2\zeta}{C}$$

$f(t)$ Arbitrary force acting on dislocation (usually – due to thermal vibration of atoms)

Three-temperature model of the radiation-induced energy spikes

$$C_e \frac{\partial T_e}{\partial t} = \kappa_e \Delta T_e - \alpha_{ep} (T_e - T_p) - \alpha_{ed} (T_e - T_d) + Q_j$$

$$C_p \frac{\partial T_p}{\partial t} = \kappa_p \Delta T_p + \alpha_{ep} (T_e - T_p) + \alpha_{dp} (T_d - T_p) + Q_p$$

$$C_d \frac{\partial T_d}{\partial t} = \kappa_d \Delta T_d + \alpha_{ed} (T_e - T_d) - \alpha_{dp} (T_d - T_p) + Q_d$$

$$\alpha_{ep} \approx \frac{m \cdot s^2 \cdot n}{T_p \cdot \tau_{ep}}$$

electron-phonon coupling

$$\alpha_{ed} \approx \frac{m \cdot s^2 \cdot n}{\omega_d \cdot \tau_{ed}}$$

electron-dislocation coupling

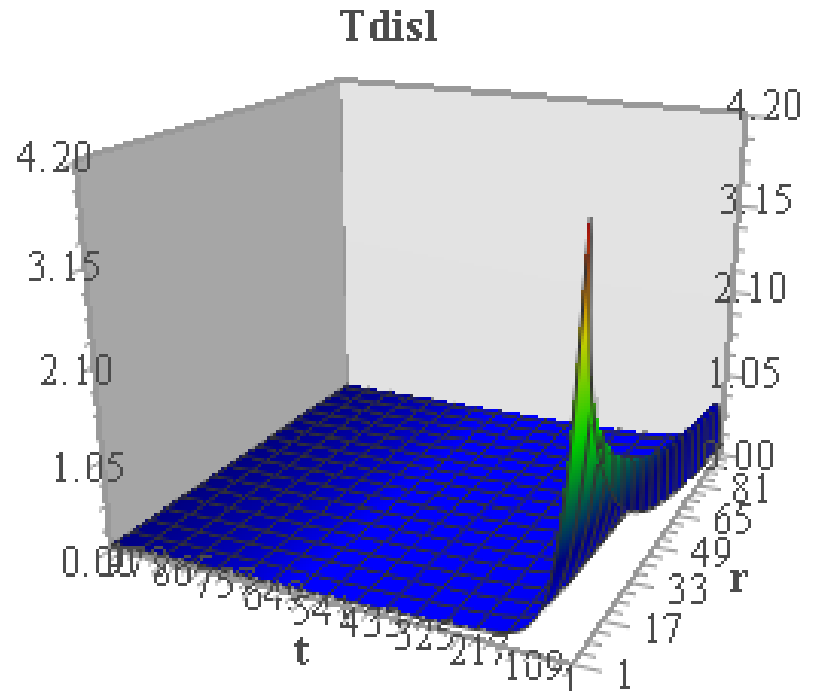
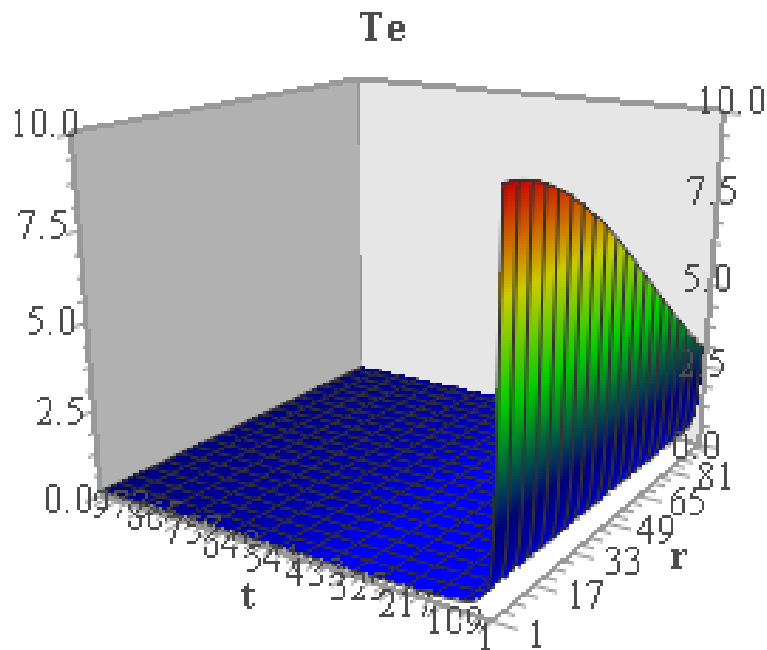
$$\alpha_{dp} \approx \frac{s \cdot C_d}{\lambda_p}$$

dislocation-phonon coupling

Radiation-induced “energy” peaks in metals: electrons vs. dislocations

$$c_e \frac{\partial T_e}{\partial t} = \kappa_e \Delta T_e - \alpha(\rho_d)(T_e - T_d)$$

$$c_d(\rho_d) \frac{\partial T_d}{\partial t} = \alpha(\rho_d)(T_e - T_d)$$



Summary

- Mechanical properties of materials **under irradiation** are different from those **under post-irradiation tests**, which should be taken into account in **forecasting the lifetime of nuclear power plants**.
- Nonequilibrium fluctuations of energy states of the atoms surrounding crystal defects arise as a result of their interaction with radiation-induced **DBs** and **quodons**. These fluctuations result in **radiation-induced recovery processes** such as the void shrinkage and ordering, saturation and even reduction of swelling, radiation-induced softening. So the **quodon mechanics** should be taken into account in **modeling of material response to irradiation**.

THANK YOU FOR YOUR ATTENTION!